Research Square

Preprints are preliminary reports that have not undergone peer review.
They should not be considered conclusive, used to inform clinical practice,
or referenced by the media as validated information.

Enhanced reactivity of the CuO-Fe2O3 intimate hetero-junction for the oxidation of quinoline yellow dye (E104)

Djedjiga Bousalah
Centre de Recherche Scientifique et Technique en Analyses Physico-Chimiques
Hanane Zazoua
CRAPC: Centre de Recherche Scientifique et Technique en Analyses Physico-Chimiques
Amel Boudjemaa (amel_boudjemaa@yahoo.fr)
research center CRAPC https://orcid.org/0000-0001-7429-6922
Abdelbaki Benmounah
Universite de Boumerdes: Universite M'Hamed Bougara Boumerdes
Mohamed Zine Messaoud-Boureghda
Universite de Boumerdes: Universite M'Hamed Bougara Boumerdes
Khaldoun Bacharı
Centre de Recherche Scientifique et Technique en Analyses Physico-Chimiques

Research Article

Keywords: quinoline yellow, CuO/Fe2O3, intimate hetero-junction, hydrogen peroxide, heterogeneous catalysis

Posted Date: February 4th, 2022

DOI: https://doi.org/10.21203/rs.3.rs-1276158/v1

License: This work is licensed under a Creative Commons Attribution 4.0 International License.
Read Full License

Abstract

This research work was designed to study the elimination of quinoline yellow (QY) in aqueous solutions by the heterogeneous Fenton and photo-Fenton processes in the presence of CuO/Fe_2O_3 photocatalyst. CuO/Fe_2O_3 derived from LDH structure was synthesized by the co-precipitation method. The physiochemical characteristics of CuO/Fe_2O_3 are des cribed by XRD, TEM/SEM, BET surface area, FTIR and pH_{PZC}.The effects of pH, H_2O_2 concentration, dye concentration, catalyst dose, reaction temperature, and reusability of catalyst on the QY decolorization efficiency were studied. The results indicated that a complete removal of QY was achieved within 150 min when the H_2O_2 and QY concentrations were 27.6 mM and 100 mg/L, respectively. The rate constants for QY removal by the heterogeneous Fenton system were calculated and the experimental data were found to fit the pseudo-first order model. Under optimal conditions, the rate constants were respectively 0.02032 and 0.02016 min^{-1} for the photo-Fenton and Fenton systems, this means that the addition of light has no significant effect.

1. Introduction

A wide variety of colors from natural and synthetic origin are added to food products in order to make them more aesthetic to consumers and to restore their original appearance, lost during the production process. However, most dyes obtained from natural sources are unstable and can easily degrade during food processing. On the other hand, the dyes of synthetic origin are widely used, not only because of their stability, but also because of their very low production cost compared to those of natural origin (Saleh et al. 2016; Yamjala et al. 2016). Therefore, It is difficult to remove the synthetic dyes from the industrial effluent, because they are stable to light and heat, and biologically non-degradable.

The presence of dyes in aqueous ecosystems decreases photosynthesis by preventing the penetration of light into deeper layer by deteriorating the quality of the water and reducing the solubility of the gas. In addition, the dyes and/or their degradation products can be toxic to flora and fauna (Bhatia 2017; Abdul Rahman et al. 2018). Hence, the conventional methods used in sewage treatment, such as the primary and secondary treatment systems, are unsuitable. Therefore, it is necessary to use tertiary treatment to remove them Nassar and Magdy (1997). Advanced oxidation processes (AOP's), like Fenton and photo-Fenton processes, could be a good option to treat and eliminate dyes. These processes appear to have the capacity to completely decolorize and partially mineralize the textile industry dyes in short reaction time Lucas and Peres (2006).

The heterogeneous advanced oxidation processes use heterogeneous catalysts to degrade organic pollutants, among of the catalysts used for heterogeneous oxidation such as metallic oxides (oxides of Mn (Zhang et al. 2012), Fe (Zhang et al. 2019), Co, Cu (Shen et al. 2015), Ni (Huo et al. 2020), Zn (Miao et al. 2014)…, and mixed metal oxides) were also used to improve the catalyst by taking advantage of the best properties of each metal (Deutschmann et al. 2009). Iron oxides have been the most studied metal oxides because they have high surface reactivity and magnetic properties and they are also environmentally friendly. they have been combined with copper to obtain a mixed oxide catalyst with

improved photocatalytic properties which can overcome the disadvantages of single metal containing oxides. However, the synthesis of bimetallic copper-iron catalysts has proven their effectiveness for degradation or even mineralization (Sun et al. 2020).

several works have been published on the preparation methods of CuO/Fe_2O_3 catalysts and their applications in different fields, notably those of dyes photodegradation (Alp et al. 2019; **Sukma Hayati AE. 2019)**, and the thermal decomposition of ammonium perchlorate (Hao et al. 2019), catalytic decomposition of H_2O_2 (Amin et al. 2016), CO removal and oxidation **(Lamai 2014)**, low-temperature carbon monoxide oxidation (Cao et al. 2008), n-hexane oxidation (Todorova et al. 2010), catalytic decomposition of H_2O_2 (Amin et al. 2016), methyl orange degradation with assistance of oxydol under irradiation of visible light and for p-nitrophenol electrocatalytic reduction in a basic solution (Pan et al. 2013). The Cu/Fe based materials have also been used Adsorption and catalytic combustion of acid red B (Wu et al. 2003), the thermal decomposition of ammonium perchlorate and the combustion of ammonium perchlorate-based propellant (Wang et al. 2010), and the p-nitrophenol electrocatalytic reduction in a basic solution (Pan et al. 2013).

Quinoline yellow (QY) named also: E104, CI Food Yellow 13, C.I. 47005 is a quinophthalone dye consisting of a mixture of disulfonates (80%), monosulfonates (15%), and trisulfonates (7%) as sodium salts. QY is obtained by the sulfonation of 2-(2-quinolyl)-1, 3indandione. with a formula of $C_{18}H_9NNa_2O_8S_2$ is a yellow powder or granules, soluble in water, sparingly soluble in ethanol. It is not permitted as food colorant in the US (Socaciu 2008).

QY is one of the most widely used in the food coloration (Damant 2011). It's used to provide a more appetizing, attractive appearance to enhance the color, taste and flavor of foods (Güray et al., 2020). It is also used in drug and cosmetic industries (Güray et al., 2020), jellies, caramels, processed seafood (e.g. caviar), lipsticks, hair products, colognes, liquors, and a wide range of medications Macioszek and Kononowicz (2004), as a synthetic colouring agent in food and drink products, as well as in cosmetics and the textile (Popa et al., 2017), for dyeing wool, silk and nylon Björkner and Niklasson (1983). However, studies have shown that QY can cause dermatitis and allergic reactions in some individuals Björkner and Niklasson (1983). It also exhibits genotoxicity which causes damage to human DNA if metabolized or absorbed through the skin (Macioszek and Kononowicz (2004); Zhao et al. 2011; Chequer et al. 2015) and leads to increased hyperactivity in children aged 8 to 9 years (McCann et al. 2007). For these reasons the use of QY in foods and medicines has been excluded in some country as Australia, USA, Norway and Japan (Macioszek and Kononowicz (2004); Roy et al. 2018), but it is still used in many countries around the world.

Several processes have been suggested for removal of QY from wastewater including, zinc oxide nanoparticle loaded on activated carbon (ZnO–NP–AC) in presence and absence of Na and K doping, used for simultaneous ultrasound-assisted (Karimi et al. 2019), photocatalytic degradation by Ag_3PO_4 (Tab et al. 2020), photocatalytic degradation in TiO_2 and ZnO aqueous suspensions (Regulska et al. 2016), ultrafiltration using polymeric membranes prepared with surfactants (Popa et al. 2017), adsorption

and desorption studies using waste materials (Gupta et al. 2005), photo-degradation catalyzed by TiO_2 (Gupta et al. 2012), removal from solutions and sludges by using polyelectrolytes and polyelectrolyte–surfactant complexes Petzold and Schwarz (2006), photocatalytic degradation with polyaniline/TiO_2 nanocomposite (Salem et al., 2009), and electrochemical sensor based on carbon nanotube-modified electrode (Zhao et al. 2011).

In this work, we are interested in the catalytic performance of the CuO/Fe_2O_3 composite synthesized by co-precipitation method with an initial atomic ratio Cu^{2+}/Fe^{3+} = 2:1, in alkaline medium, followed by the calcination of 600°C, for 4 h to produce the intimate hetero-junction CuO/Fe_2O_3. It has been used in the catalytic degradation of QY in the presence of hydrogen peroxide. The effect of various parameters including: pH, H_2O_2 concentration, dye concentration, the catalyst dose and its reuse, the irradiation and the temperature on the degradation kinetics was evaluated and discussed.

2. Experimental

2.1. Analytical Reagents

All chemicals and reagents; Tartrazine (high purity biological stain), Iron (III) nitrate nonahydrate ($Fe(NO_3)_3$. $9H_2O$, 98%, Panreac), Copper(II) Nitrate Hexahydrate ($Cu(NO_3)_2$. $3H_2O$, 99%) were supplied by Merck, hydrogen peroxide (H_2O_2, 30%, VWR Chemicals), hydrochloric acid (HCl, 37%, Analar Normaour VWR Prolabo chemicals) and sodium hydroxide (NaOH, 85–100%, Biochim Chimo pharma) were used without any purification.

2.2 Catalyst preparation

The CuO/Fe_2O_3 composite was synthesized by co-precipitation method. 5 g $Cu(NO_3)_2$, $6H_2O$ and 4.18 g $Fe(NO_3)_3$, $9H_2O$ (initial atomic ratio Cu^{2+}/Fe^{3+} = 2:1) were dissolved into 50 mL distilled water, and the other containing a NaOH (1N). Then, two solutions were mixed together with vigorous stirring at room temperature until the pH at approximately 10 by adjusting the flow of this solution. The suspension, thus obtained was kept at 60°C for 15 h. The precipitate was filtered and washed with deionised water until pH ~ 7 of the filtrate and then dried at 70°C for 24h. Finally, the obtained precursor was calcined at a constant heating rate of 5°C. min^{-1} up to 600°C for 4h to produce the CuO/Fe_2O_3.

2.3. Characterization techniques

The chemical composition and scanning electron microscopy (SEM) of the material was determined by EDX FEI QUANTA F Environmental apparatus equipped a back-scatter detector (BSE) at 15 kV. The crystallization phase of sample obtained was studied using powder X-ray diffraction (PXRD). The analysis was carried out in a Siemens D-5000 diffractometer with a monochromator, using CuKα radiation (λ = 0.154056 nm) over a range of 5–70° (2θ), with step of 0.05° and 2S by step. The Infra-red spectra were obtained a using FTIR spectrophotometer (Alpha Bruker FTIR). Samples were prepared by mixing the powdered solids with potassium bromide, KBr (the blank) in 15:85 ratio to get transparent

pellet auto supported on the different solids at 10 ton pressure. The infrared spectra were recorded both over the wave number range from 4000 to 400 cm^{-1}. The textural characteristics, such as BET specific area, pore volume and average pore diameter (BJH method) were determined using conventional nitrogen adsorption/desorption method at -196°C in a Micromeritics Tristar 3000. Prior to nitrogen adsorption, the sample was outgassed for 8 h at 250°C to evacuate the physically adsorbed moisture. Scanning electron microscopy (SEM) experiment was performed with a Zeiss Supra 55 VP FEG microscope with an acceleration voltage of 30 kV. Transmission electron microscopy (TEM) was carried out on a JEOL JEM-2000EX-II instrument at an accelerating voltage of 120 Kv, the sample was dispersed in ethanol, and carbon-coated copper grids were used as the sample holder. The positive or negative dimensions of ZP are determined by identifying which electrode the particles are moving towards during electrophoresis. Sample concentration was 0.1g/100 mL in distillated water. The sample was transferred to a zeta cell and measured at 25°C using a ZetaSizer 2000 (Malvern instruments) and an applied voltage of 150 V. To determine the pH value at the point of zero charge (pH_{PZC}), pH tests were carried out by a simple and rapid method which consists of placing 50 cm^3 of 0.01 M NaCl solution in closed flasks and adjusting the pH of each (values between 2 and 12) by adding NaOH or HCl solution (0.1 M), 0.15 g was added to the adsorbent. The suspensions must be kept in constant stirring, at room temperature, for 48 h, in order to determine the final pH. The pH_{PZC} is the point where the pH_{final} vs. pHinitial intercepts the line pH_{final} = $pH_{initial}$.

2.4. Heterogeneous Fenton degradation of QY dye

The degradation tests of the quinoline (E104) were performed during a series of experiments in batch method at temperature of 20°C. In this oxidation tests, 100 ml of QY (100 mg/L) was maintained under continuous stirring (250 rpm), hydrogen peroxide was injected simultaneously with the material. This latter step was considered as t_0 (time zero). The samples were collected in each 15 min and analysis by a UV/visible spectrometer (T60 UV/Vis, PG. Instruments) at 413 nm.

3. Results And Discussion

3.1. Characterization

The stœchiometry of the synthesized Cu/Fe was verified by the SEM/EDX analysis. The molar fraction of the cations Cu^{2+}/Fe^{3+} in the sheet are reported in Table 1. As it can be seen, the Cu^{2+}/Fe^{3+} atomic ratio was similar to that expected. The powder X-ray diffraction patterns (PXRD) of Cu/Fe is shown in Fig. 1. The typical peaks indexed with 2θ approximately at 35°, 38°, 48°, 53°, 58°, 61° and 66°, which were attributed of CuO phase (JCPDS 05-0661) whereas those at 2θ = 24°, 33°, 41°, 56°, 63° and 68° indicate the presence of Fe_2O_3 (JCPDS 39-1346). The FTIR spectrum of the CuO/Fe_2O_3 shows absorption bands at 3428 and 1647 cm^{-1} were ascribed to the O–H stretching mode (νO–H) and to the HOH deformation mode (δH–O–H), respectively (Ohnishi et al. 2007) (Fig. 2). The bands at 475 cm^{-1} was ascribed to CuO vibration, whereas that at 578 cm^{-1} corresponding to the Fe^{3+} and O^{2-} bonds stretching in the FeO_4

tetrahedron (Hao et al. 2015). The adsorption–desorption isotherms of the CuO/Fe_2O_3 was presented in Fig. 3. According to the International Union of Pure and Applied Chemistry classification, the sample exhibited type IV adsorption isotherms with a hysteresis loop in the relative pressure region around 0.4-0.9, which is a characteristic of mesoporous materials (Sing 1985). The BET specific surface areas and the pore diameter calculated by the Barrett–Joyner–Halenda (BJH) theory of the sample was listed in **Table 1**. The morphology of the CuO/Fe_2O_3 was revealed by SEM (Fig. 4-a). The CuO/Fe_2O_3 sample consists of many irregular spherical grains of different colours; these observations confirm the formation of oxide mixtures CuO/Fe_2O_3. TEM image of the CuO/Fe_2O_3 composite is shown in Fig. 4-b, it observed that CuO/Fe_2O_3 is composed by two different morphology particles, where several Fe_2O_3 hexagonal morphology can be observed on and around the CuO spherical structure. For the zeta potential (ZP), the averaged (over five measurements) was (- 38.96 mV), which may indicate the presence of a negative charge on the surface of the CuO/Fe_2O_3 catalyst. A negative surface charge favors the adsorption of cationic and basic dyes, which can be explained by the increased electrostatic attraction force (Guedes et al. 2009). The pH_{PZC} of catalyst is 9 (Fig. 5) This makes its charge positive for a lower pH and negative for a higher pH.

3.2. Catalytic degradation

3.2.1. Effect of pH

Heterogeneous Fenton oxidation is one of the advanced oxidation processes which has gained wide spread acceptance for higher removal efficiency of pollutants under wide range of pH compared to homogeneous reactions (S Atalay 2016). The catalytic degradation of QY (100 ml, 100 ppm), $[H_2O_2]_0$ = 27.6 mM, by CuO/Fe_2O_3 (0.01 g/L) was studied by varying pH in the range [3–10]. The pH value affects the oxidation of organic substances both directly and indirectly. The Fenton reaction is strongly pH dependent. The pH value influences the generation of HO° and thus the oxidation efficiency (Behnajady et al. 2007). The results illustrated on Fig. 6 indicated that the degradation of QY was significantly influenced by the pH of the solution and that the process is more efficient in acid medium. The pH = 3 shows the best rate of dye removal (100%) in 150 min, this may be due to the substantial production of HO° in the solution at this pH (Khataee and Pakdehi (2014**); Bousalah. 2019)**. Thus, the results clearly indicate that the extent and efficiency of the degradation of QY decreases with the increase in the pH value (i.e. 80.5, 64.2, 56.8 and 55.2% respectively for pH = 5, 6.5, 8 and 10 after 150 min) which may be due to the decomposition of H_2O_2 into water and oxygen **(Eq. 1)** (Szpyrkowicz et al. 2001), thus the oxidation rate decreases due to the decrease of HO° Hameed and Lee (2009).

$$2H_2O_2 \rightarrow 2\,H_2O + O_2 \quad \textbf{(Eq.1)}$$

The pHzc of catalyst is 9. This makes its charge positive for a lower pH and negative for a higher pH. The QY molecule is anionic (its mobile ion is Na^+ in basic medium and H^+ in acidic medium). For pH below 9, there is an attraction between the catalyst and dye thus promoting the catalytic action.

3.2.2. Effect of hydrogen peroxide concentration

The effect of the oxidizing agent dose on the catalytic oxidation process was investigated or the H_2O_2 concentrations from 9.2 to 55.2 mM under the following conditions: $[Dye]_0$ = 100 mg/L, pH = 3, catalyst amount = 0.01 g and at T = 20°C. The data shown in Fig. 7 shows a great influence of the concentration of H_2O_2 on the process catalyzed by CuO/Fe_2O_3. At the start of the reaction, the discoloration increases with the dose of hydrogen peroxide, this may be due to the formation of more radicals. Same oxidant effect was observed for other molecules and catalyst, in particular, those studied by Sohrabi (Hameed & Lee (2009) ; Sohrabi et al. 2014), but above 36.8 mM, the effect of H_2O_2 is not significant, in 135 minutes of reaction, it was recorded rates of 97.86, 100, 100 and 100% respectively for 27.6, 36.8, 46 and 55.2 mM because at fairly high concentrations, H_2O_2 is a powerful scavenger of HO° (Aravindhan et al. 2006; Ramirez et al., 2007; Hameed and Lee (2009)). However, the higher concentrations of H_2O_2 in the presence of additional hydroxyl radicals leads to the formation of less reactive hydroperoxyl radicals (HO_2°) and thereby decrease the yield of the dye degradation **(Eq. 2 and 3)** (Najjar et al. 2007; Hameed and Lee (2009)).

$H_2O_2 + HO° \rightarrow HO_2° + H_2O$ **(Eq. 2)**

$HO_2° + HO° \rightarrow H_2O + O_2$ **(Eq. 3)**

3.2.3. Effect of QY concentration

The effect of the initial concentration of the QY on the degradation rate was studied by varying the initial concentration of the QY from 10 to 100 mg/L under the following operating conditions: pH = 3, $[H_2O_2]_0$ = 27.6 mM, catalyst amount = 0.01 g at T = 20°C. The results reveal that increasing the QY concentration decreases the removal efficiency (Fig. 8), the discoloration rates are total for 10, 30 mg /L and are 87.15, 64.7, 61.8, 53.5% for 50, 70, 80 and 100 mg/L in 60 min.

The rate constant decreases with increasing dye concentration, i.e. values of 0.0504, 0.04108, 0.02731, 0.02541, 0.02185 and 0.02016 min^{-1} respectively for 10, 30, 50, 70, 80, 100 mg/L. This behavior is one of the characteristics of advanced oxidation processes (Daneshvar et al. 2008). The increase of initial QY concentration would decrease the probability of the reaction between QY molecules and the °OH (Zhang et al. 2009), the amount of reactive radicals is not enough to oxidize the excessive concentration of QY due to constant rate of reactive species formation on the catalyst for various concentrations of QY (Dulman et al. 2012; Khataee and Pakdehi (2014)) attributed this behavior to the limited number of °OH involved in the degradation process.

3.2.4. Effect of catalyst dose and it reuse

To clarify the role of the catalyst in the degradation of the QY by heterogeneous oxidation of the Fenton type, experiments were carried out to study the variations in the rate of discoloration at different concentrations of the catalyst, ranging from 0 to 0.4 g/L under the following experimental conditions:

100 mg/L dye, $[H_2O_2]_0$ = 27.6 mM, pH = 3, and T = 20°C. The results show that the degradation of the QY is strongly dependent on the dose of catalyst at the fixed concentration of hydrogen peroxide, QY and temperature (Fig. 9). The degradation of the QY was very slow in the absence of the catalyst, only 13.2% after 60 min. Nevertheless, an increase to 34.6% is achieved when only 0.05 g/L was added, thus demonstrating the vital role of the catalyst in the rapid formation of HO° promoted by its surface. Further increase the catalyst dose from 0.1 to 0.4 g/L, could greatly increase the QY degradation efficiency from 53.5 to 68.1% in the same time interval (60 min), The improved degradation rate may be due to the increased availability of active sites, which increases the number of QY molecules adsorbed and subsequently degraded **(**Song et al. 2008 ; Szeto et al. 2014; Sun et al. 2018; **Bousalah et al. 2019;** Hamza et al. 2020 ; **Bousalah et al. 2021)**. The kinetic study shows that the elimination of the dye by oxidation with hydrogen peroxide catalyzed by our catalyst follows the pseudo-first order (Table 2). The degradation rate constant increases from 0.00222 to 0.02066 min^{-1} for 0 and 0.4 g/L, respectively.

The stability of the catalyst was studied by the re-use of the same sample for three successive times and before each reuse, the catalyst was washed with deionized water and dried at 105°C to constant weight. The results show that the rate of QY removal decreases slightly between the first and third use (Fig. 10). At 150 min, rates of 100, 95.7, 93.6% were recorded for the first, second and third use, respectively. These values show the stability of the catalytic activity of our catalyst.

3.2.5. Effect of temperature

The effect of temperature was studied in the range of 20–40°C. The results were shown that percent QY removal on Fenton process was accelerated by a rise in temperature (Figure 11). The efficiency of QY was increased from 53.5 to 100% with increasing temperature up to 40°C in 60 min, which improved the generation rate of °OH and therefore enhancing the decolorization of the QY **(**Ertugay and Acar (2017**) ;** Sun et al. 2009), indicating that the catalytic degradation of QY is an endothermic process. This may be due to the facilitated interaction of the catalysts with H_2O_2 to yield ROS (reactive oxygen species) HO°and the accelerated molecular diffusion at higher reaction temperatures **(**Sun et al. 2018).

This is because a higher temperature increased the rate of reaction between H_2O_2 and any form of ferrous/ferric ion, thus increasing the rate of generation of oxidizing species such as the ˙OH radical or high valence iron species **(**Chen and Zhu (2007**);** Daud et al. 2010).

3.2.6. Order kinetics of removal of QY in oxidation by hydrogen peroxide

The rate constants for the elimination of QY by hydrogen peroxide catalyzed by CuO/Fe_2O_3 for the various temperatures studied were calculated and the experimental data were found to correspond to a pseudo first- order model with respect to QY. The following relation can express the rate of dye removal **(Eq. 4)**:

$- dc/dt = Kapp\ C$ (Eq. 4)

where C, t and Kapp are respectively QY concentration, time and apparent rate constant. The linear plots of ln C_0/C, where C_0 is the initial concentration of QY, versus time are plotted and Kapp was determined from the slopes (Fig. 12). The result shows that the dye removal by oxidation with hydrogen peroxide catalyzed by CuO/Fe_2O_3 follows a pseudo – first order.

The apparent rate constants Kapp and coefficient of determination R^2 at different temperature are presented in Table 3. The apparent activation energy of the dye removal by hydrogen peroxide in presence of the QY removal by hydrogen peroxide in presence of CuO/Fe_2O_3 is calculated from the linear form of the Arrhenius equation **(Eq. 5)**

$\ln Kapp = \ln K_0 - Ea/RT$ (Eq. 5)

where K_0 is the pre-exponential factor and Ea is the apparent activation energy (J. mol^{-1}); R is the ideal gas constant (8.314 J mol^{-1} K^{-1}); T is the reaction absolute temperature (K). After plotting ln Kapp as a function of 1/T (Fig. 13), the value of the apparent activation energy was determined from the slope of regression line. The apparent activation energy of catalytic decomposition of dye is 36.36 kJ/mol. The value of the activation energy found can confirm that the oxidation mechanism of QY is radical **(Bousalah et al. 2021;** Yeddou et al. 2010).

3.2.7. Photo-Fenton degradation

Figure 14 present the decoloration efficiency of QY as a function of time under two different systems Fenton and photo-Fenton. The irradiation source used for the photo-Fenton was a tungsten lamp (200 W). The results reveal a significant increase in the rate and the time of discoloration, a total degradation (100%) was recorded after 105 min in the photo-Fenton system and after 135 min in the Fenton system and under the same operating conditions, the rate constants were 0.02032 and 0.02016 min^{-1} respectively for the photo-Fenton and Fenton systems. In the photo-Fenton, the additional sources of °OH should be considered: through photolysis of H_2O_2, **Eq. (6)**, through reduction of Fe^{3+} ions under UV light, **Eq. (7)**, and through reduction of Cu^{2+} ions under UV light, **Eq. (8) (**Peternel et al. 2007). However, as it has been observed the presence of CuO plays an important role in the photo-Foton process. This result can be explained by the activation of CuO in the presence of light to generate electron-hole pairs **Taufik and Saleh (2016)**, which contribute to the degradation of QY by a photo-Fenton mechanism.

$H_2O_2 + hv \rightarrow HO° + HO°$ (Eq. 6)

$Fe^{3+} + H_2O + hv \rightarrow Fe^{2+} + HO° + H^+$ **(Eq. 7)**

$Cu^{2+} + hv \rightarrow Cu^+$ **(Eq. 8)**

4. Oxidative Degradation Mechanism “heterogeneous Fenton-like”

On the basis of all the experimental results and references of previous work, we have proposed a possible mechanism of heterogeneous Fenton-type reaction d in the $CuO/Fe_2O_3/H_2O_2$ system in the degradation of QY in **the equations (9-16)**.

H_2O_2 molecules absorbed on the inner surface of CuO/Fe_2O_3 can reduce Fe^{3+} to Fe^{2+} ions according to the Fenton-type process, and the formed Fe^{2+} ions can react with Cu^{2+} ions to generate Cu^{+} and Fe^{2+} ions **(Eq 9 and 10) (Li et al. 2016)**. Thus, the Cu^{+} and Fe^{3+} ions react with other H_2O_2 molecules to promote the generation of highly active HO° for dye degradation **(Eq 11 and 12) (Li et al. 2016)**. These equations explain the exceptional performance of bimetallic catalysts, due to the presence of Cu and Fe as two catalytically active sites that can generate larger amounts of the HO° radicals responsible for dye degradation. On the other hand, the excess of H_2O_2 can react with Cu^{2+}/Fe^{3+} ions to form Cu^{2+}-H_2O_2 and Fe^{3+}-H_2O_2 complexes and generate HO_2° **(eq 13 and 14) (** Jin et al. 2017). These equations can explain that the further increase of H_2O_2 dosage leads to the production of HO_2° radicals, which are less active than HO° radicals.

$Fe^{3+} + H_2O_2 \rightarrow Fe^{2+} + H^{+} + HO_2$° (Eq. 9)

$Fe^{2+} + Cu^{2+} \rightarrow Fe^{3+} + Cu^{+}$ **(Eq. 10)**

$Cu^{+} + H_2O_2 \rightarrow Cu^{2+} + OH^{-} + HO$° **(Eq. 11)**

$Fe^{2+} + H_2O_2 \rightarrow Fe^{3+} + OH^{-} + HO$° **(Eq. 12)**

Fe^{3+}–O-O– $Fe^{3+} + 2H_2O_2 \rightarrow Fe^{2+}$–O-O– $Fe^{2+} + 2HO_2$° $+ 2H^{+}$ **(Eq. 13)**

Cu^{2+}–O-O– $Cu^{2+} + 2H_2O_2 \rightarrow Cu^{+}$–O-O– $Cu^{+} + 2HO_2$° $+ 2H^{+}$ **(Eq. 14)**

HO° + dye → degradation products **(Eq. 15)**

HO_2° + dye → degradation products **(Eq. 16)**

Conclusion

CuO/Fe_2O_3 hetero-junction was prepared by a simple co-precipitated process and examined by different analytical techniques. It was found to be a low-cost and efficient catalyst for Fenton Fenton like oxidation reaction, especially for the degradation of QY in aqueous solution. In the optimum condition of: 27.6 mM of H_2O_2, and 100 mg/L of dye, pH = 3, 0.01 g of the catalyst at 20°C, the decolorization efficiency of 53.5 and 100% was achieved within 60 and 150 min of reaction, respectively. The kinetics study indicated that the decolorization kinetics of QY followed the first-order kinetics. Most importantly, the regeneration of the photocatalyst is quite easy and have excellent recyclability (93.6%) even after three consecutive cycles.

The apparent activation energy Ea, for the decolorization of QY by Fenton oxidation was determined to be 36.36 kJ mol^{-1}.

Declarations

Acknowledgments

This work is supported by the Directorate-General for Scientific Research and Technological

Development DGRSDT and they are thanked for their financial support.

Disclosure statement

No conflict of interest to declare.

References

1. Alp E, Eşgin H, Kazmanlı MK, Genç A (2019) Synergetic activity enhancement in 2D CuO-Fe2O3 nanocomposites for the photodegradation of rhodamine B. Ceram Int 45:9174–9178. doi:10.1016/j.ceramint.2019.01.258
2. Amin NH, Ali LI, El-Molla SA, Ebrahim AA, Mahmoud HR (2016) Effect of Fe2O3 precursors on physicochemical and catalytic properties of CuO/Fe2O3 system. Arabian Journal of Chemistry 9:S678–S684. doi:10.1016/j.arabjc.2011.07.026
3. Aravindhan R, Fathima NN, Rao JR, Nair BU (2006) Wet oxidation of acid brown dye by hydrogen peroxide using heterogeneous catalyst Mn-salen-Y zeolite: A potential catalyst. J Hazard Mater 138:152–159. doi:10.1016/j.jhazmat.2006.05.052
4. Ardiansyah Taufik RS (2017) Synthesis of iron(II,III) oxide/zinc oxide/copper(II) oxide (Fe3O4/ZnO/CuO) nanocomposites and their photosonocatalytic property for organic dye removal. J Colloid Interface Sci 491:27–36. doi:10.1016/j.jcis.2016.12.018
5. Behnajady MA, Modirshahla N, Ghanbary F (2007) A kinetic model for the decolorization of C.I. Acid Yellow 23 by Fenton process. J Hazard Mater 148:98–102. doi:10.1016/j.jhazmat.2007.02.003
6. Björkner B, Niklasson B (1983) Contact allergic reaction to D & C Yellow No. 11 and Quinoline Yellow. Contact Dermat 9:263–268. doi:10.1111/j.1600-0536.1983.tb04387.x
7. Bousalah.Dj YAR, Hachemi M, Nadjemi B (2019) Removal of methylene blue in aqueous solution by oxidation with hydrogen peroxide in presence of copper-impregnated activated alumina. Algerian Journal of Environmental Science and Technology 5:7
8. Cao J-L, Wang Y, Yu X-L, Wang S-R, Wu S-H, Yuan Z-Y (2008) Mesoporous CuO–Fe2O3 composite catalysts for low-temperature carbon monoxide oxidation. Appl Catal B 79:26–34. doi:10.1016/j.apcatb.2007.10.005

9. Chen J, Zhu L (2007) Heterogeneous UV-Fenton catalytic degradation of dyestuff in water with hydroxyl-Fe pillared bentonite. Catal Today 126:463–470. doi:10.1016/j.cattod.2007.06.022
10. Chequer FMD, Venâncio VdP, de Souza Prado MR, Junior LR, Lizier TM, Zanoni MVB, Rodríguez Burbano R, Bianchi MLP, Antunes LMG (2015) The cosmetic dye quinoline yellow causes DNA damage in vitro. Mutation Research/Genetic Toxicology and Environmental Mutagenesis 777: 54-61. doi:10.1016/j.mrgentox.2014.11.003
11. Damant AP (2011) Food colourants. 252-305. doi:10.1533/9780857094919.2.252
12. Daneshvar N, Aber S, Vatanpour V, Rasoulifard MH (2008) Electro-Fenton treatment of dye solution containing Orange II: Influence of operational parameters. J Electroanal Chem 615:165–174. doi:10.1016/j.jelechem.2007.12.005
13. Daud NK, Ahmad MA, Hameed BH (2010) Decolorization of Acid Red 1 dye solution by Fenton-like process using Fe–Montmorillonite K10 catalyst. Chem Eng J 165:111–116. doi:10.1016/j.cej.2010.08.072
14. Djedjiga Bousalah ARY, Messaoud Hachemi A, Chergui B Nadjemi (2021) OXIDATION OF AZO DYE CARMOISINE (E122) IN AQUEOUS SOLUTION BY HETEROGENEOUS CATALYST CuO/Al2O3 SYSTEM. Environ Eng Manag J 20:9
15. Dulman V, Cucu-Man SM, Olariu RI, Buhaceanu R, Dumitraş M, Bunia I (2012) A new heterogeneous catalytic system for decolorization and mineralization of Orange G acid dye based on hydrogen peroxide and a macroporous chelating polymer. Dyes Pigm 95:79–88. doi:10.1016/j.dyepig.2012.03.024
16. Ertugay N, Acar FN (2017) Removal of COD and color from Direct Blue 71 azo dye wastewater by Fenton's oxidation: Kinetic study. Arabian Journal of Chemistry 10:S1158–S1163. doi:10.1016/j.arabjc.2013.02.009
17. Guedes M, Ferreira JMF, Ferro AC (2009) Dispersion of Cu2O particles in aqueous suspensions containing 4,5-dihydroxy-1,3-benzenedisulfonic acid disodium salt. Ceram Int 35:1939–1945. doi:10.1016/j.ceramint.2008.10.023
18. Gupta VK, Jain R, Agarwal S, Nayak A, Shrivastava M (2012) Photodegradation of hazardous dye quinoline yellow catalyzed by TiO2. J Colloid Interface Sci 366:135–140. doi:10.1016/j.jcis.2011.08.059
19. Gupta VK, Mittal A, Gajbe V (2005) Adsorption and desorption studies of a water soluble dye, Quinoline Yellow, using waste materials. J Colloid Interface Sci 284:89–98. doi:10.1016/j.jcis.2004.09.055
20. Güray T, Menevşe B, Yavuz AA (2020) Determination of optimization parameters based on the Box-Behnken design for cloud point extraction of quinoline yellow using Brij 58 and application of this method to real samples. Spectrochim Acta Part A Mol Biomol Spectrosc 243:118800. doi:10.1016/j.saa.2020.118800
21. Hameed BH, Lee TW (2009) Degradation of malachite green in aqueous solution by Fenton process. J Hazard Mater 164:468–472. doi:10.1016/j.jhazmat.2008.08.018

22. Hamza M, Altaf AA, Kausar S, Murtaza S, Rasool N, Gul R, Badshah A, Zaheer M, Ali Shah SA, Zakaria ZA (2020) Catalytic Removal of Alizarin Red Using Chromium Manganese Oxide Nanorods: Degradation and Kinetic Studies. Catalysts 10:1150. doi:10.3390/catal10101150
23. Hang Jin XT, Yulun Nie Z, Zhou C, Yang Y, Li, Lu L (2017) Oxygen Vacancy Promoted Heterogeneous Fentonlike Degradation of Ofloxacin at pH 3.2-9.0 by Cu Substituted Magnetic Fe3O4@FeOOH Nanocomposite. Environmental Science & Technology: 34. doi:10.1021/acs.est.7b04503
24. Hao C, Feng F, Wang X, Zhou M, Zhao Y, Ge C, Wang K (2015) The preparation of Fe2O3 nanoparticles by liquid phase-based ultrasonic-assisted method and its application as enzyme-free sensor for the detection of H2O2. RSC Adv 5:21161–21169. doi:10.1039/c4ra17226d
25. Hao G, Li H, Mao C, Hu Y, Xiao L, Zhang G, Liu J, Jiang W, Zhao F, Gao H (2019) Preparation of Nano-Cu-Fe Composite Metal Oxides via a Mechanical Grinding Method and Its Catalytic Performance for the Thermal Decomposition of Ammonium Perchlorate. Combust Sci Technol 1–18. doi:10.1080/00102202.2019.1679125
26. Huo X, Zhou P, Zhang J, Wei C, Liu Y, Zhang G, Li W, Zhang Y (2020) Synthetic NiO catalyst-assisted peroxymonosulfate for degradation of benzoic acid from aqueous solution. Water Environ Res. doi:10.1002/wer.1336
27. Hao C, Feng F, Wang X, Zhou M, Zhao Y, Ge C, Wang K (2015) The preparation of Fe_2O_3 nanoparticles by liquid phase-based ultrasonic-assisted method and its application as enzyme-free sensor for the detection of H_2O_2, R S C Advances.1–24
28. Igor T, Peternel NK, Ana M, Lonˇcari´c Boˇzi´c, Hrvoje M, Kuˇsi´c (2007) Comparative study of UV/TiO2, UV/ZnO and photo-Fenton processes for the organic reactive dye degradation in aqueous solution. J Hazard Mater 148:8
29. Karimi R, Yousefi F, Ghaedi M, Rezaee Z (2019) Comparison the behavior of ZnO–NP–AC and Na, K doped ZnO–NP–AC for simultaneous removal of Crystal Violet and Quinoline Yellow dyes: Modeling and optimization. Polyhedron 170:60–69. doi:10.1016/j.poly.2019.05.038
30. Khataee AR, Pakdehi SG (2014) Removal of sodium azide from aqueous solution by Fenton-like process using natural laterite as a heterogeneous catalyst: Kinetic modeling based on nonlinear regression analysis. J Taiwan Inst Chem Eng 45:2664–2672. doi:10.1016/j.jtice.2014.08.007
31. Lamai W, Aunbamrung P, Wongkaew A (2014) Characteristic and Catalytic activity of CuO supported over Fe2O3 catalyst for CO removal: International Conference 2014 Burapha University, Thailand (ed
32. Lucas M, Peres J (2006) Decolorization of the azo dye Reactive Black 5 by Fenton and photo-Fenton oxidation. Dyes Pigm 71:236–244. doi:10.1016/j.dyepig.2005.07.007
33. MACIOSZEK RKKaVK (2004) THE EVALUATION OF THE GENOTOXICITY OF TWO COMMONLY USED FOOD COLORS: QUINOLINE YELLOW (E 104) AND BRILLIANT BLACK BN (E 151). CELLULAR & MOLECULAR BIOLOGY LETTERS 9: 17
34. Magda MS, Saleh EYH, Najat OA, Al-Salahi (2016) Oxidation and Complexation-Based Spectrophotometric Methods for Sensitive Determination of Tartrazine E102 in Some Commercial Food Samples. Computational Chemistry 4:14

35. Mahmood R, Sohrabi AKa S, Shariati S Shariati (2014) Removal of Carmoisine edible dye by Fenton and photo Fenton processes using Taguchi orthogonal array design. Arabian Journal of Chemistry 10:9
36. McCann D, Barrett A, Cooper A, Crumpler D, Dalen L, Grimshaw K, Kitchin E, Lok K, Porteous L, Prince E, Sonuga-Barke E, Warner JO, Stevenson J (2007) Food additives and hyperactive behaviour in 3-year-old and 8/9-year-old children in the community: a randomised, double-blinded, placebo-controlled trial. The Lancet 370:1560–1567. doi:10.1016/s0140-6736(07)61306-3
37. Miao J, Jia Z, Lu H-B, Habibi D, Zhang L-C (2014) Heterogeneous photocatalytic degradation of mordant black 11 with ZnO nanoparticles under UV–Vis light. J Taiwan Inst Chem Eng 45:1636–1641. doi:10.1016/j.jtice.2013.11.007
38. Rahman MNasriA (2018) NAAR, Wan Farahiyah Wan Kamarudin, Zildawarni Irwan, Abd Rahman Mat Amin, Adida Muhammud, Siti Munirah Muda, Noor Erni Fazlina Mohd. Akhir Solar Photocatalytic Degradation of Food Dye (Tartrazine) using Zinc Oxide Catalyst. International Journal of Engineering & Technology 7: 4
39. Najjar W, Azabou S, Sayadi S, Ghorbel A (2007) Catalytic wet peroxide photo-oxidation of phenolic olive oil mill wastewater contaminants. Appl Catal B 74:11–18. doi:10.1016/j.apcatb.2007.01.007
40. Nassar MM, Magdy YH (1997) Removal of different basic dyes from aqueous solutions by adsorption on palm-fruit bunch particles. Chem Eng J 66:223–226. doi:10.1016/s1385-8947(96)03193-2
41. Ohnishi M, Kusachi I, Kobayashi S, Yamakawa J (2007) Mineral chemistry of schulenbergite and its Zn-dominant analogue from the Hirao mine, Osaka, Japan. J Mineral Petrol Sci 102:233–239. doi:10.2465/jmps.061130
42. OLAF DEUTSCHMANN HK KARLKOCHLOEFL, THOMAS TUREK (2009) Heterogeneous Catalysis and Solid Catalysts. Ullmann's Encyclopedia of Industrial Chemistry 110. doi:10.1002/14356007.a05_313.pub2
43. Pan L, Tang J, Wang F (2013) Facile synthesis of nanoscaled α-Fe2O3, CuO and CuO/Fe2O3 hybrid oxides and their electrocatalytic and photocatalytic properties. Open Chemistry 11:763–773. doi:10.2478/s11532-013-0207-6
44. Petzold G, Schwarz S (2006) Dye removal from solutions and sludges by using polyelectrolytes and polyelectrolyte–surfactant complexes. Sep Purif Technol 51:318–324. doi:10.1016/j.seppur.2006.02.016
45. Popa GA, Enache DF, Tanczos SK, Ciocanea A (2017) Ultrafiltration of Aqueous Solutions of Food Dye Using Polymeric Membranes Prepared with Surfactants. Materiale Plastice 54:726–730
46. Ramirez JH, Maldonado-Hódar FJ, Pérez-Cadenas AF, Moreno-Castilla C, Costa CA, Madeira LM (2007) Azo-dye Orange II degradation by heterogeneous Fenton-like reaction using carbon-Fe catalysts. Appl Catal B 75:312–323. doi:10.1016/j.apcatb.2007.05.003
47. Regulska E, Brus DM, Rodziewicz P, Sawicka S, Karpinska J (2016) Photocatalytic degradation of hazardous Food Yellow 13 in TiO2 and ZnO aqueous and river water suspensions. Catal Today

266:72–81. doi:10.1016/j.cattod.2015.08.010

48. Roy U, Manna S, Sengupta S, Das P, Datta S, Mukhopadhyay A, Bhowal A (2018) Dye Removal Using Microbial Biosorbents 19:253–280. doi:10.1007/978-3-319-92162-4_8
49. Atalay S (2016) EG Novel Catalysts in Advanced Oxidation of Organic Pollutants: SpringerBriefs in Molecular Science, GREEN CHEMISTRY FOR SUSTAINABILITY (ed. by J Sanjay K. Sharma, India), p. 69
50. Bhatia SC, Sarvesh D (2017) Pollution Control in Textile Industry. WOODHEAD PUBLISHING INDIA PVT LTD, New Delhi, India
51. Salem MA, Al-Ghonemiy AF, Zaki AB (2009) Photocatalytic degradation of Allura red and Quinoline yellow with Polyaniline/TiO2 nanocomposite. Appl Catal B 91:59–66. doi:10.1016/j.apcatb.2009.05.027
52. Shen Y, Zhang Z, Xiao K (2015) Evaluation of cobalt oxide, copper oxide and their solid solutions as heterogeneous catalysts for Fenton-degradation of dye pollutants. RSC Adv 5:91846–91854. doi:10.1039/c5ra18923c
53. Silviya Todorova J-LC, Paneva D, Tenchev K, Mitov I, Kadinov G, Yuan Z-Y (2010) Vasko Idakiev Mesoporous CuO-Fe2O3 composite catalysts for complete n-hexane oxidation: 10th International Symposium “Scientific Bases for the Preparation of Heterogeneous Catalysts”Elsevier B.V. All rights reserved MD EM, Gaigneaux S, Hermans P, Jacobs J, Martens, Ruiz P (eds)), p. 4
54. Socaciu C (2008) Chemical and Functional Properties of Food Components Series. 2008 by Taylor & Francis Group, LLC, Boca Raton London New York
55. Song S, Xu L, He Z, Ying H, Chen J, Xiao X, Yan B (2008) Photocatalytic degradation of C.I. Direct Red 23 in aqueous solutions under UV irradiation using SrTiO3/CeO2 composite as the catalyst. J Hazard Mater 152:1301–1308. doi:10.1016/j.jhazmat.2007.08.004
56. Sukma Hayati AER, and Ramli (2019) Semiconductor-Based Photocatalysts Degradation of Methyl Orange Using Cuo-Fe2O3 Nanocomposites.International Journal of Progressive Sciences and Technologies (IJPSAT)15 5
57. Sun B, Li H, Li X, Liu X, Zhang C, Xu H, Zhao XS (2018) Degradation of Organic Dyes over Fenton-Like Cu2O–Cu/C Catalysts. Ind Eng Chem Res 57:14011–14021. doi:10.1021/acs.iecr.8b02697
58. Sun M, Lei Y, Cheng H, Ma J, Qin Y, Kong Y, Komarneni S (2020) Mg doped CuO–Fe2O3 composites activated by persulfate as highly active heterogeneous catalysts for the degradation of organic pollutants. J Alloys Compd 825:154036. doi:10.1016/j.jallcom.2020.154036
59. Sun S-P, Li C-J, Sun J-H, Shi S-H, Fan M-H, Zhou Q (2009) Decolorization of an azo dye Orange G in aqueous solution by Fenton oxidation process: Effect of system parameters and kinetic study. J Hazard Mater 161:1052–1057. doi:10.1016/j.jhazmat.2008.04.080
60. Szeto W, Kan CW, Yuen CWM, Chan S-W, Lam KH (2014) Effective Photodegradation of Methyl Orange Using Fluidized Bed Reactor Loaded with Cross-Linked Chitosan Embedded Nano-CdS Photocatalyst. International Journal of Chemical Engineering 2014:1–16. doi:10.1155/2014/270946

61. Szpyrkowicz L, Juzzolino C, Kaul SN (2001) A Comparative study on oxidation of disperse dyes by electrochemical process, ozone, hypochlorite and fenton reagent. Water Res 35:2129–2136. doi:10.1016/s0043-1354(00)00487-5
62. Tab A, Dahmane M, Chemseddin B, Bellal B, Trari M, Richard C (2020) Photocatalytic Degradation of Quinoline Yellow over Ag3PO4. Catalysts 10:1461. doi:10.3390/catal10121461
63. Wang Y, Xia X, Zhu J, Li Y, Wang X, Hu X (2010) Catalytic Activity of Nanometer-Sized CuO/Fe2O3on Thermal Decompositon of AP and Combustion of AP-Based Propellant. Combust Sci Technol 183:154–162. doi:10.1080/00102202.2010.507561
64. Wu R (2003) Adsorption and catalytic combustion of ARB on CuO-Fe2O3. Chin Sci Bull 48:2311. doi:10.1360/03wb0083
65. Xiaoming Li YK, Shijian Zhou, Wang B (2016) In situ incorporation of well-dispersed Cu–Fe oxides in the mesochannels of AMS and their utilization as catalysts towards the Fenton-like degradation of methylene blue. J Mater Sci 52:14. doi:10.1007/s10853-016-0436-0
66. Yamjala K, Nainar MS, Ramisetti NR (2016) Methods for the analysis of azo dyes employed in food industry – A review. Food Chem 192:813–824. doi:10.1016/j.foodchem.2015.07.085
67. Yeddou AR, Nadjemi B, Halet F, Ould-Dris A, Capart R (2010) Removal of cyanide in aqueous solution by oxidation with hydrogen peroxide in presence of activated carbon prepared from olive stones. Miner Eng 23:32–39. doi:10.1016/j.mineng.2009.09.009
68. Zhang H, Fu H, Zhang D (2009) Degradation of C.I. Acid Orange 7 by ultrasound enhanced heterogeneous Fenton-like process. J Hazard Mater 172:654–660. doi:10.1016/j.jhazmat.2009.07.047
69. Zhang Y, Yang Y, Zhang Y, Zhang T, Ye M (2012) Heterogeneous oxidation of naproxen in the presence of α-MnO2 nanostructures with different morphologies. Appl Catal B 127:182–189. doi:10.1016/j.apcatb.2012.08.014
70. Zhang Y, Zhang N, Wang T, Huang H, Chen Y, Li Z, Zou Z (2019) Heterogeneous degradation of organic contaminants in the photo-Fenton reaction employing pure cubic β-Fe2O3. Appl Catal B 245:410–419. doi:10.1016/j.apcatb.2019.01.003
71. Zhao J, Zhang Y, Wu K, Chen J, Zhou Y (2011) Electrochemical sensor for hazardous food colourant quinoline yellow based on carbon nanotube-modified electrode. Food Chem 128:569–572. doi:10.1016/j.foodchem.2011.03.067
72. Yamjala K, Nainar MS, Ramisetti NR (2016) Methods for the analysis of azo dyes employed in food industry – A review. Food Chem 192:813–824. http://dx.doi.org/10.1016/j.foodchem.2015.07.085
73. Saleh MMS, Hashem EY, Al-Salahi NOA (2016) Oxidation and Complexation-Based Spectrophotometric Methods for Sensitive Determination of Tartrazine E102 in Some Commercial Food Samples. J Comput Chem 4:14–64. http://dx.doi.org/10.4236/cc.2016.42005
74. Bhatia SC (2007) Pollution Control in Textile Industry. New Delhi, India
75. Abdul Rahman MN, Abd Rahim NA, Wan Kamarudin WF, Irwan Z, Mat Amin AR, Muhammud A, Muda SM, NEFM Akhir((2018) Solar Photocatalytic Degradation of Food Dye (Tartrazine) using Zinc Oxide

Cataly. Int J Eng Technol 7:222–226. http://dx.doi.org/10.14419/ijet.v7i4.42.25719

76. Nassar MM, Magdy YH (1997) Removal of different basic dyes from aqueous solutions by adsorption on palm-fruit bunch particles. Chem Eng J 66:223–226. doi:10.1016/s1385-8947(96)03193-2
77. Lucas M, JPeres (2006) Decolorization of the azo dye Reactive Black 5 by Fenton and photo-Fenton oxidation. Dyes Pigm 71:236–244. doi:10.1016/j.dyepig.2005.07.007
78. Zhang Y, Yang Y, Zhang Y, Zhang T, Ye M (2012) Heterogeneous oxidation of naproxen in the presence of α-MnO2 nanostructures with different morphologies. Appl Catal B: Environ 127:182–189. http://dx.doi.org/10.1016/j.apcatb.2012.08.014
79. Zhang Y, Zhang N, Wang T, Huang H, Chen Y, Li Z, Zou Z (2019) Heterogeneous degradation of organic contaminants in the photo-Fenton reaction employing pure cubic β-Fe2O3. Appl Catal B: Environ 245:410–419. https://doi.org/10.1016/j.apcatb.2019.01.003
80. Shen Y, Zhang Z, Xiao K (2015) Evaluation of cobalt oxide, copper oxide and their solid solutions as heterogeneous catalysts for Fenton-degradation of dye pollutants. R S C Adv 5:91846–91854. http://dx.doi.org/10.1039/c5ra18923c
81. Huo X, Zhou P, Zhang J, Wei C, Liu Y, Zhang G, Li W, Zhang Y (2020) Synthetic NiO catalyst-assisted peroxymonosulfate for degradation of benzoic acid from aqueous solution. Water Resour Res 1–10. http://dx.doi.org/10.1002/wer.1336
82. Miao J, Jia Z, Lu HB, Habibi D, Zhang LC (2013) Heterogeneous photocatalytic degradation of mordant black 11 with ZnO nanoparticles under UV–Vis ligh. J Taiwan Inst Chem Eng 45:1636–1641. http://dx.doi.org/10.1016/j.jtice.2013.11.007
83. Deutschmann O, Ozinger H, Kochloefl K, Turek T (2009) Classification of Solid Catalysts. Heterogeneous Catalysis and Solid Catalysts. Ullmann's Encyclopedia of Industrial Chemistry. Wiley-VCH Verlag GmbH & Co. KGaA, Weinhei
84. Sun M, Lei Y, Cheng H, Ma J, Qin Y, Kong Y, Komarneni S (2020) Mg doped CuO–Fe2O3 composites activated by persulfate as highly active heterogeneous catalysts for the degradation of organic pollutants. J Alloys Compd 825:1–10. https://doi.org/10.1016/j.jallcom.2020.154036
85. Alp E, Eşgin H, Kazmanlı MK, A Genç (2019) Synergetic activity enhancement in 2D CuO-Fe_2O_3 nanocomposites for the photodegradation of rhodamine B. Ceram Int 45:9174–9178. https://doi.org/10.1016/j.ceramint.2019.01.258
86. Hayati AES, Ratnawulan R (2019) Semiconductor-Based Photocatalysts Degradation of Methyl Orange Using Cuo-Fe2O3 Nanocomposites. Int J Adv Sci Technol 15:1–5
87. Hao G, Li H, Mao C, Hu Y, Xiao L, Zhang G, Liu J, Jiang W, Zhao F, Gao H (2019) Preparation of Nano-Cu-Fe Composite Metal Oxides via a Mechanical Grinding Method and Its Catalytic Performance for the Thermal Decomposition of Ammonium Perchlorate. Combust Sci Technol 1–18. https://doi.org/10.1080/00102202.2019.1679125
88. Amin NH, Ali LI, El-Molla SA, Ebrahim AA, Mahmoud HR (2016) Effect of Fe2O3 precursors on physicochemical and catalytic properties of CuO/Fe2O3 system. Arab J Chem 9:S678–S684.

http://dx.doi.org/10.1016/j.arabjc.2011.07.026

89. Lamai W, Aunbamrung P, Wongkaew A (2014) Characteristic and Catalytic activity of CuO supported over Fe_2O_3 catalyst for CO removal, International Conference Burapha University, Thailand
90. Cao JL, Wang Y, Yu XL, Wang SR, Wu SH, ZY Yuan (2008) Mesoporous CuO–Fe_2O_3 composite catalysts for low-temperature carbon monoxide oxidation. Appl Catal B: Environ 79:26–34. http://dx.doi.org/10.1016/j.apcatb.2007.10.005
91. Todorova S, Caob JL, Panevaa D, Tencheva K, Mitova I, Kadinova G, Yuanb ZY, Idakieva V (2010) Mesoporous CuO-Fe_2O_3 composite catalysts for complete n-hexane oxidation. In: E.M. Gaigneaux, M. Devillers, S. Hermans, P. Jacobs, J. Martens and P. Ruiz (Editors)© 2010 Elsevier B.V. All rights reserved.10th International Symposium “Scientific Bases for the Preparation of Heterogeneous Catalysts”Elsevier BV All rights reserved, p. 4
92. Pan L, Tang J, Wang F (2013) Facile synthesis of nanoscaled α-Fe_2O_3, CuO and CuO/Fe_2O_3 hybrid oxides and their electrocatalytic and photocatalytic properties. Cent Eur J Chem 11:763–773. http://dx.doi.org/10.2478/s11532-013-0207-6
93. Wu R, Qu J, He H, Yu Y (2003) Adsorption and catalytic combustion of ARB on CuO-Fe_2O_3. Chin Sci Bull 48:2311–2316. http://dx.doi.org/10.1360/03wb0083
94. Wang Y, Xia X, Zhu J, Li Y, Wang X, X Hu (2010) Catalytic Activity of Nanometer-Sized CuO/Fe2O3on Thermal Decompositon of AP and Combustion of AP-Based Propellant. Combust Sci Technol 183:154–162. http://dx.doi.org/10.1080/00102202.2010.507561
95. C Socaciu Chemical and Functional Properties of Food Components Series, Boca Raton London New York, Taylor & Francis Group
96. AP Damant (2011) Food colourants, © Woodhead Publishing Limited, pp 252–305
97. Güray T, Menevşe B, Yavuz AA (2020) Determination of optimization parameters based on the Box-Behnken design for cloud point extraction of quinoline yellow using Brij 58 and application of this method to real samples. Spectrochim Acta - A: Mol Biomol Spectrosc 243:118–124. https://doi.org/10.1016/j.saa.2020.118800
98. Macioszek VK, Kononowicz AK (2004) The evaluation of the genotoxicity of two commonly used food colors: quinoline yellow (E 104) and brilliant black BN (EC151). Cell Mol Biol Lett 9:107–122
99. Popa GA, Enache DF, Tanczos SK, ACiocanea (2017) Ultrafiltration of aqueous solutions of food dye using polymeric membranes prepared with surfactants. Mater Plast 54:726–730. http://dx.doi.org/10.37358/mp.17.4.4932
100. Björkner B, Niklasson B (1983) Contact allergic reaction to D & C Yellow No. 11 and Quinoline Yellow. Contact Derm 9:263–268. http://dx.doi.org/10.1111/j.1600-0536.1983.tb04387.x
101. Zhao J, Zhang Y, Wu K, Chen J, Zhou Y (2011) Electrochemical sensor for hazardous food colourant quinoline yellow based on carbon nanotube-modified electrode. Food Chem 128:569–572. https://doi.org/10.1016/j.foodchem.2011.03.067

102. Drumond Chequer FM, Venâncio VP, Prado MRS, Juniorc LRCSC, Lizier TM, Zanonid MVB, Burbano RR, Bianchia MLP, Antunesa LMG (2014) The cosmetic dye quinoline yellow causes DNA damage in vitro. Mutat Res Genet Toxicol Environ Mutagen 777:54–61. https://doi.org/10.1016/j.mrgentox.2014.11.003
103. McCann D, Barrett A, Cooper A, Crumpler D, Dalen L, Grimshaw K, Kitchin E, Lok K, Porteous L, Prince E, Sonuga-Barke E, Warner JO, Stevenson J Food additives and hyperactive behaviour in 3-year-old and 8/9-year-old children in the community: a randomised, double-blinded, placebo-controlled trial,Lancet.70:1560–1567. http://dx.doi.org/10.1016/S0140-6736(07)61306-3
104. Roy U, Manna S, Sengupta S, Das P, Datta S, Mukhopadhyay A, Bhowal A (2018) Dye Removal Using Microbial Biosorbents, © Springer Nature Switzerland AG, pp 254–273
105. Karimi R, Yousefi F, Ghaedi M, Rezaee Z (2019) Comparison the behavior of ZnO–NP–AC and Na, K doped ZnO–NP–AC for simultaneous removal of Crystal Violet and Quinoline Yellow dyes: Modeling and optimization. Polyhedron 170:60–69. https://doi.org/10.1016/j.poly.2019.05.038
106. Tab A, Dahmane M, Chemseddin B, Bellal B, Trari M, C Richard (2020) Photocatalytic Degradation of Quinoline Yellow over Ag_3PO_4. Catalysts 10:1461. http://dx.doi.org/10.3390/catal10121461
107. Regulska E, Brus DM, Rodziewicz P, Sawicka S, Karpinska J (2016) Photocatalytic degradation of hazardous Food Yellow 13 in TiO2 and ZnO aqueous and river water suspensions. Catal Today 266:72–81. http://dx.doi.org/10.1016/j.cattod.2015.08.010
108. Gupta VK, Mittal A, V Gajbe (2005) Adsorption and desorption studies of a water soluble dye, Quinoline Yellow, using waste materials. J Colloid Interface Sci 284:89–98. http://dx.doi.org/10.1016/j.jcis.2004.09.055
109. Gupta VK, Jain R, Agarwal S, Nayak A, Shrivastava M (2012) Photodegradation of hazardous dye quinoline yellow catalyzed by TiO_2. J Colloid Interface Sci 366:135–140. http://dx.doi.org/10.1016/j.jcis.2011.08.059
110. Petzold G, Schwarz S (2006) Dye removal from solutions and sludges by using polyelectrolytes and polyelectrolyte–surfactant complexes. Sep Purif Technol 51:318–324. http://dx.doi.org/10.1016/j.seppur.2006.02.016
111. Salem MA, Al-Ghonemiy AF, Zaki AB (2009) Photocatalytic degradation of Allura red and Quinoline yellow with Polyaniline/TiO_2 nanocomposite. Appl Catal B: Environ 91:59–66. http://dx.doi.org/10.1016/j.apcatb.2009.05.027
112. Ohnishi M, Kusachi I, Kobayashi S, J Yamakawa (2007) Mineral chemistry of schulenbergite and its Zn-dominant analogue from the Hirao mine, Osaka, Japan. J Mineral Petrol Sci 102:233–239. http://dx.doi.org/10.2465/jmps.061130
113. Hao C, Feng F, Wang X, Zhou M, Zhao Y, Ge C, Wang K (2015) The preparation of Fe_2O_3 nanoparticles by liquid phase-based ultrasonic-assisted method and its application as enzyme-free sensor for the detection of H_2O_2. R S C Advances. 5:21161–21169. http://dx.doi.org/10.1039/c4ra17226d

114. Sing KSW, Everett DH, Haul RAW, Moscou L, Pierotti RA, Rouquerol J, Siemieniewska T (1985) Reporting physisorption data for gas/solid systems with special reference to the determination of surface area and porosity (Recommendations 1984). Pure & App Chem 57:603–619. http://dx.doi.org/10.1351/pac198557040603
115. Guedes M, Ferreira JMF, Ferro AC (2009) Dispersion of Cu_2O particles in aqueous suspensions containing 4,5-dihydroxy-1,3-benzenedisulfonic acid disodium salt. Ceram Int 35:1939–1945. http://dx.doi.org/ 10.1016/j.ceramint.2008.10.023
116. Atalay S, Ersöz G (2016) Novel catalysts in advanced oxidation of organic pollutants, In: Sanjay K. Sharma J, India, editor. SpringerBriefs in Molecular Science, Green chemistry for sustainability, p. 69. http://dx.doi.org/ 10.1007/978-3-319-28950-2 (eBook)
117. Behnajady MA, Modirshahla N, Ghanbary F (2007) A kinetic model for the decolorization of C.I. Acid Yellow 23 by Fenton process. J Hazard Mater 148:98–102. doi:10.1016/j.jhazmat.2007.02.003
118. Dj Bousalah AR, Yeddou M, Hachemi B, Nadjemi (2019) Removal of methylene blue in aqueous solution by oxidation with hydrogen peroxide in presence of copper-impregnated activated alumina. Algerian J Env Sc Technology 5:983–989
119. Dj Bousalah AR, Yeddou M, Hachemi A, Chergui B, Nadjemi (2021) Oxidation of azo dye carmoisine (E122) in aqueous solution by heterogeneous catalyst CuO/Al_2O_3 system. Environ Eng Manag J 20:167–175
120. Karatas M, Argun YA, Argun ME (2012) Decolorization of antraquinonic dye, Reactive Blue 114 from synthetic wastewater by Fenton process: Kinetics and thermodynamics. J Ind Eng Chem 18:1058–1062. http://dx.doi.org /10.1016/j.jiec.2011.12.007
121. Khataee AR, Zarei M, Khatae AR (2011) Heterogeneous catalytic degradation of cyanide using copper-impregnated pumice and hydrogen peroxide. Clean - Soil Air Water 39:482–490. http://dx.doi.org /10.1002/clen.201000120
122. Khataee AR, Pakdehi SG (2014) Removal of sodium azide from aqueous solution by Fenton-like process using natural laterite as a heterogeneous catalyst: Kinetic modeling based on nonlinear regression analysis. J Taiwan Inst Chem Eng 45:2664–2672. http://dx.doi.org/10.1016/j.jtice.2014.08.007
123. Szpyrkowicz L, Juzzolino C, Kaul SN (2001) A Comparative study on oxidation of disperse dyes by electrochemical process, ozone, hypochlorite and fenton reagent. Wat Res 35:2129–2136. http://dx.doi.org/10.1016/s0043-1354(00)00487-5
124. Hameed BH, Lee TW (2009) Degradation of malachite green in aqueous solution by Fenton process. J Hazard Mater 164:468–472. http://dx.doi.org/10.1016/j.jhazmat.2008.08.018
125. Sohrabi MR, Khavaran A, Shariati S, Shariati S (2014) Removal of Carmoisine edible dye by Fenton and photo Fenton processes using Taguchi orthogonal array design. Arabian J Chem 10:S3523–S3531. http://dx.doi.org/10.1016/j.arabjc.2014.02.019
126. Aravindhan R, Fathima NN, Rao JR, Nair BU Wet oxidation of acid brown dye by hydrogen peroxide using heterogeneous catalyst Mn-salen-Y zeolite: A potential catalyst,J Hazard Mater B138:152–159.

http://dx.doi.org/10.1016/j.jhazmat.2006.05.052

127. Ramirez JH, Maldonado-Ho´dar FJ, Pe´rez-Cadenas AF, Moreno-Castilla C, Costa CA, Madeira LM (2007) Azo-dye Orange II degradation by heterogeneous Fenton-like reaction using carbon-Fe catalysts. Appl Catal B: Environ 75:312–323. http://dx.doi.org/10.1016/j.apcatb.2007.05.003
128. Najjar W, Azabou S, Sayadi S (2007) A Ghorbel, Catalytic wet peroxide photo-oxidation of phenolic olive oil mill wastewater contaminants. Appl Catal B: Environ 74:11–18. http://dx.doi.org/10.1016/j.apcatb.2007.01.007
129. Daneshvar N, Aber S, Vatanpour V, MH Rasoulifard (2008) Electro-Fenton treatment of dye solution containing Orange II: Influence of operational parameters. J Electroanal Chem 615:165–174. http://dx.doi.org/10.1016/j.jelechem.2007.12.005
130. Zhang H, Fu H, Zhang D (2009) Degradation of C.I. Acid Orange 7 by ultrasound enhanced heterogeneous Fenton-like process. J Hazard Mater 172:654–660. http://dx.doi.org/10.1016/j.jhazmat.2009.07.047
131. Dulman V, Cucu-Man SM, Olariu RI, Buhaceanu R, Dumitraş M, Bunia I (2012) A new heterogeneous catalytic system for decolorization and mineralization of Orange G acid dye based on hydrogen peroxide and a macroporous chelating polymer. Dyes Pigm 95:79–88. http://dx.doi.org/10.1016/j.dyepig.2012.03.024
132. Sun B, Li H, Li X, Liu X, Zhang C, Xu H, Zhao XS (2018) Degradation of Organic Dyes over Fenton-Like Cu2O–Cu/C Catalysts. Ind Eng Chem Res 57:14011–14021. http://dx.doi.org/10.1021/acs.iecr.8b02697
133. Szeto W, Kan CW, Yuen CWM, Chan SW, Lam KH (2014) Effective Photodegradation of Methyl Orange Using Fluidized Bed Reactor Loaded with Cross-Linked Chitosan Embedded Nano-CdS Photocatalyst. Int J Chem Eng 1–16. http://dx.doi.org/10.1155/2014/270946
134. Muhammad H, Altaf AA, Kausar S, Murtaza S, Rasool N, Gul R, Badshah A, Zaheer M, Shah SAA, Zakaria ZA (2020) Catalytic removal of alizarin red using chromium manganese oxide nanorods: degradation and kinetic studies. Catalysts 10:1–17. http://dx.doi.org/10.3390/catal10101150
135. Song S, Xu L, He Z, Ying H, Chen J, Xiao X, B Yan (2008) Photocatalytic degradation of C.I. Direct Red 23 in aqueous solutions under UV irradiation using SrTiO3/CeO2 composite as the catalyst. J Hazard Mater 152:1301–1308. http://dx.doi.org/10.1016/j.jhazmat.2007.08.004
136. Ertugay N, Acar FN (2017) Removal of COD and color from Direct Blue 71 azo dye wastewater by Fenton's oxidation: Kinetic study. Arab J Chem 10:S1158–S1163. http://dx.doi.org/10.1016/j.arabjc.2013.02.009
137. Sun SP, Li CJ, Sun JH, Shi SH, Fan MH, Zhou Q (2009) Decolorization of an azo dye Orange G in aqueous solution by Fenton oxidation process: Effect of system parameters and kinetic study. J Hazard Mater 161:1052–1057. http://dx.doi.org/10.1016/j.jhazmat.2008.04.080
138. Chen J, Zhu L (2007) Heterogeneous UV-Fenton catalytic degradation of dyestuff in water with hydroxyl-Fe pillared bentonite. Catal Today 126:463–470. http://dx.doi.org/10.1016/j.cattod.2007.06.022

139. Daud NK, Ahmad MA, Hameed BH (2010) Decolorization of Acid Red 1 dye solution by Fenton-like process using Fe–Montmorillonite K10 catalyst. Catal Today 165:111–116. http://dx.doi.org/10.1016/j.cej.2010.08.072

140. Yeddou AR, Nadjemi B, Halet F, Ould-Dris A, Capart R (2010) Removal of cyanide in aqueous solution by oxidation with hydrogen peroxide in presence of activated carbon prepared from olive stones. Miner Eng 23:32–39. http://dx.doi.org/10.1016/j.mineng.2009.09.009

141. Peternel IT, Koprivanac N, Boˇzi´c AML, HM Kuˇsi´c (2007) Comparative study of UV/TiO2, UV/ZnO and photo-Fenton processes for the organic reactive dye degradation in aqueous solution. J Hazard Mater 148:477–484. http://dx.doi.org/10.1016/j.jhazmat.2007.02.072

142. Ardiansyah T, Rosari S (2017) Synthesis of iron(II,III) oxide/zinc oxide/copper(II) oxide (Fe_3O_4/ZnO/CuO) nanocomposites and their photosonocatalytic property for organic dye removal. J Colloid Interface Sci 1–21. http://dx.doi.org/10.1016/j.jcis.2016.12.018

143. Li X, Kong Y, Zhou S, Wang B (2017) In situ incorporation of well-dispersed Cu–Fe oxides in the mesochannels of AMS and their utilization as catalysts towards the Fenton-like degradation of methylene blue. J Mater Sci 52:1432–1445. 10.1007/s10853-016-0436-0

144. Jin H, Tian X, Nie Y, Zhou Z, Yang C, Li Y, Lu L (2017) Oxygen Vacancy Promoted Heterogeneous Fentonlike Degradation of Ofloxacin at pH 3.2-9.0 by Cu Substituted Magnetic Fe_3O_4@FeOOH Nanocomposite. Environ Sci Technol 1–34. DOI: 10.1021/acs.est.7b04503

Tables

Table.1 Chemical composition and textural properties of Cu/Fe sample

Sample	Cu-Fe-LDH
Theorical ratio Cu^{2+}/Fe^{3+}	2
Cu^{2+}/Fe^{3+} molar ratio	1.80
BET surface area (cm^2/g)	9
Langnuim surface area (m^2/g)	13
BJH pore volume (cm^3/g)	0.022
BJH pore size (nm)	12
Crystallite size (nm)	23.18

Table 2

Apparent rate constant K and correlation coefficient R^2 of the elimination of quinoline yellow (E104) by hydrogen peroxide at different doses of catalyst.

Dose du catalyseur (g/L)	0	0,05	0,1	0,2	0,3	0,4
R^2	0,99914	0,92366	0,92729	0,9319	0,94074	0,95228
K (min^{-1})	0,00222	0,01183	0,01686	0,0177	0,01924	0,02066

Table 3. Apparent rate constants Kapp and coefficient of determination R^2 of dye removal by hydrogen peroxide at different temperature.

	Pseudo-first order	
T(°K)	k(min^{-1})	R^2
293	0.01715	0.93349
298	0.01993	0.9021
303	0.02267	0.91876
308	0.03294	0.93877
313	0.0441	0.99689

Figures

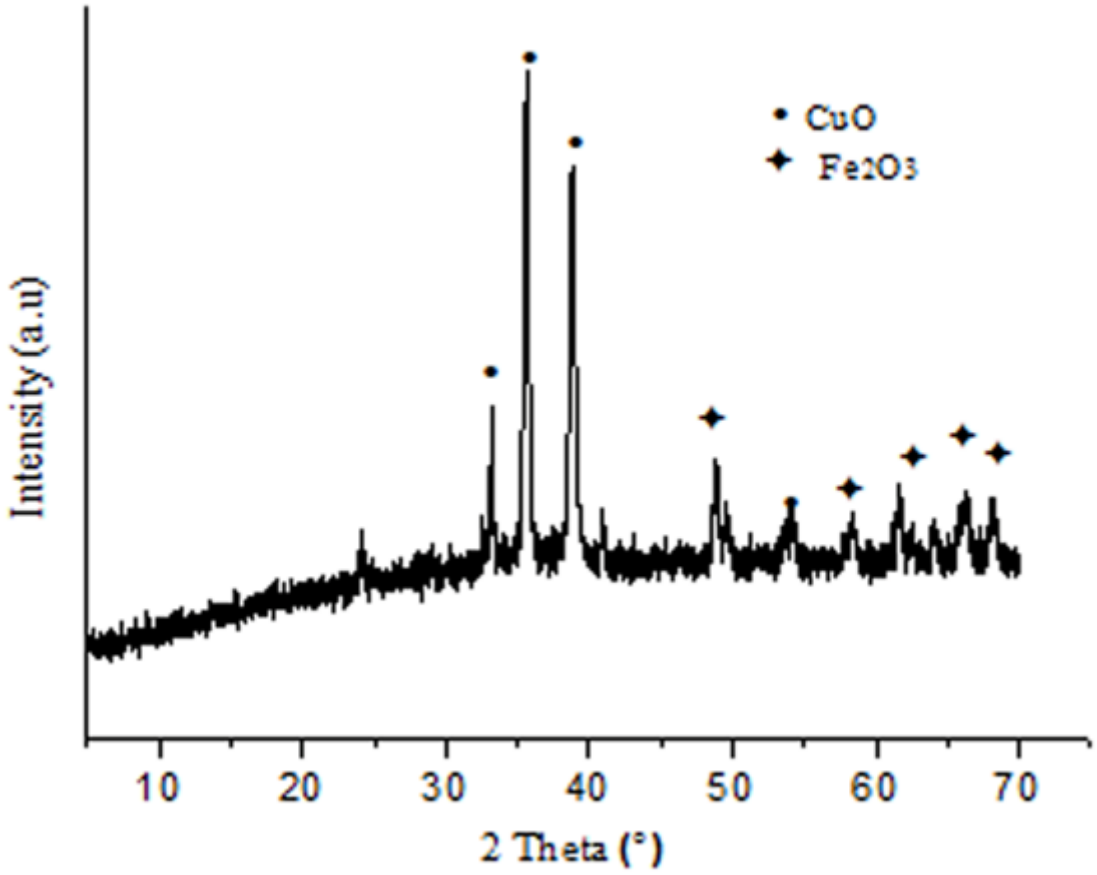

Figure 1

XRD patterns for Cu/Fe sample

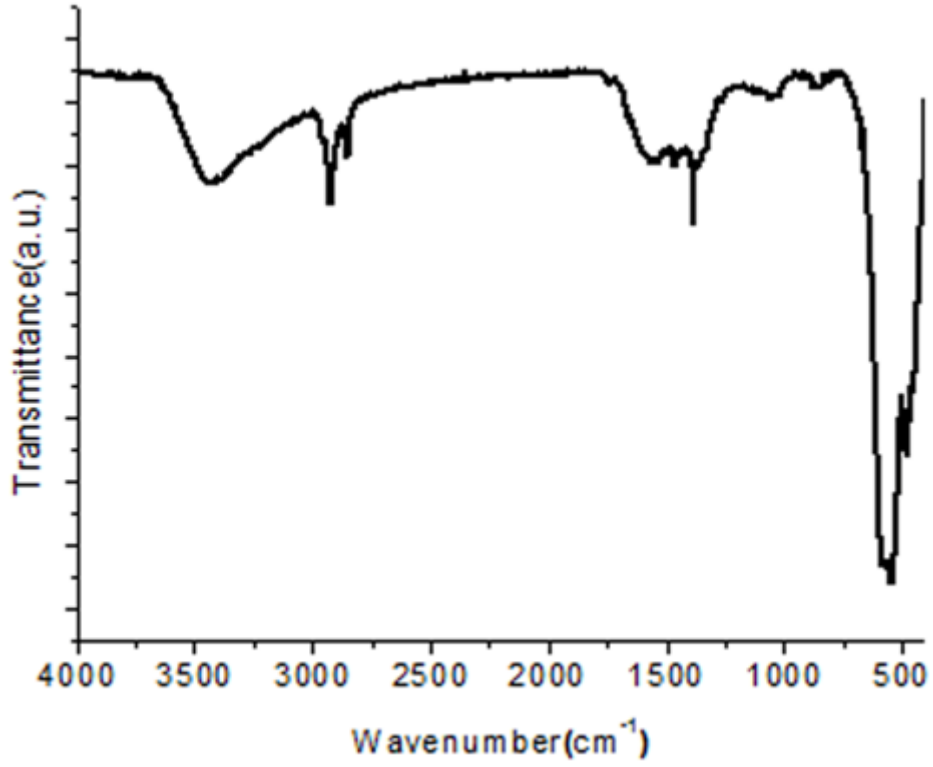

Figure 2

FT-IR spectra of Cu/Fe sample

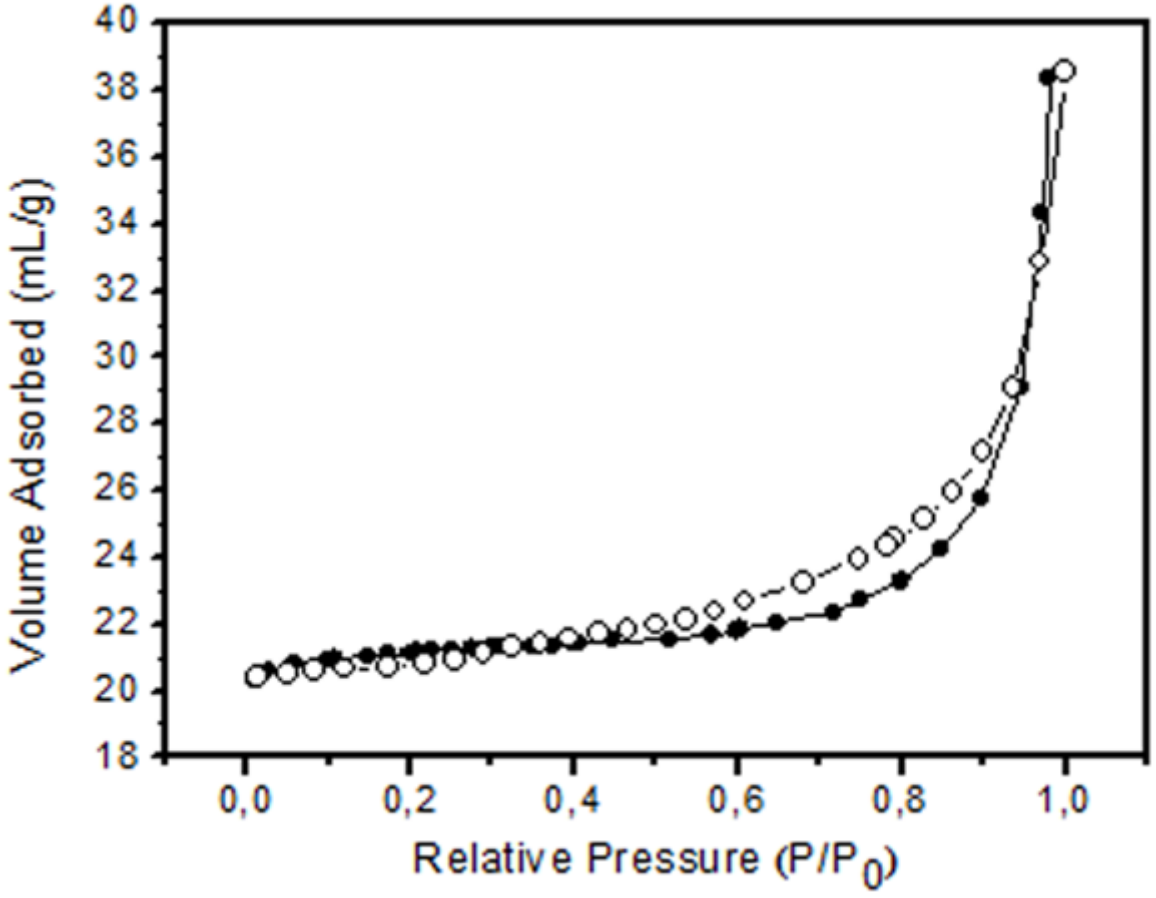

Figure 3

The adsorption–desorption isotherm for Cu/Fe sample

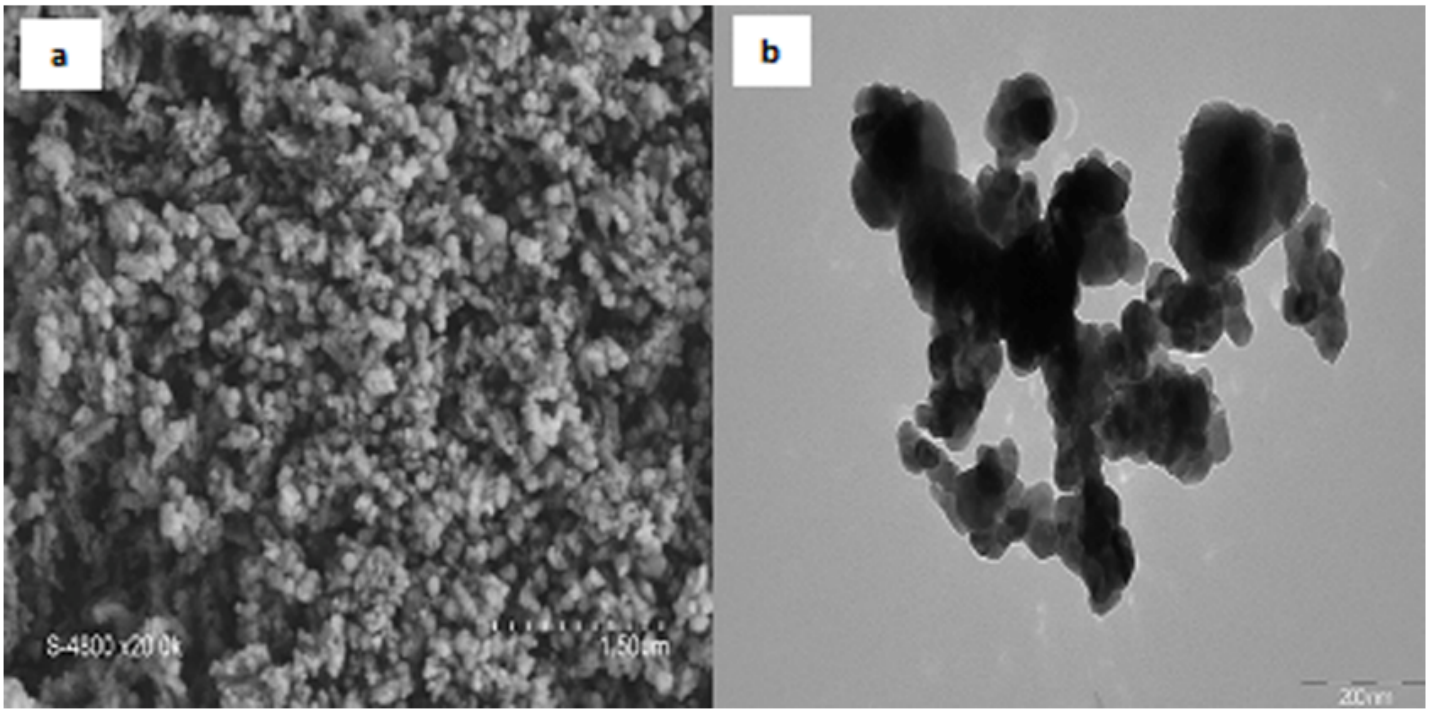

Figure 4

(a-b) SEM and TEM images of CuO/Fe_2O_3

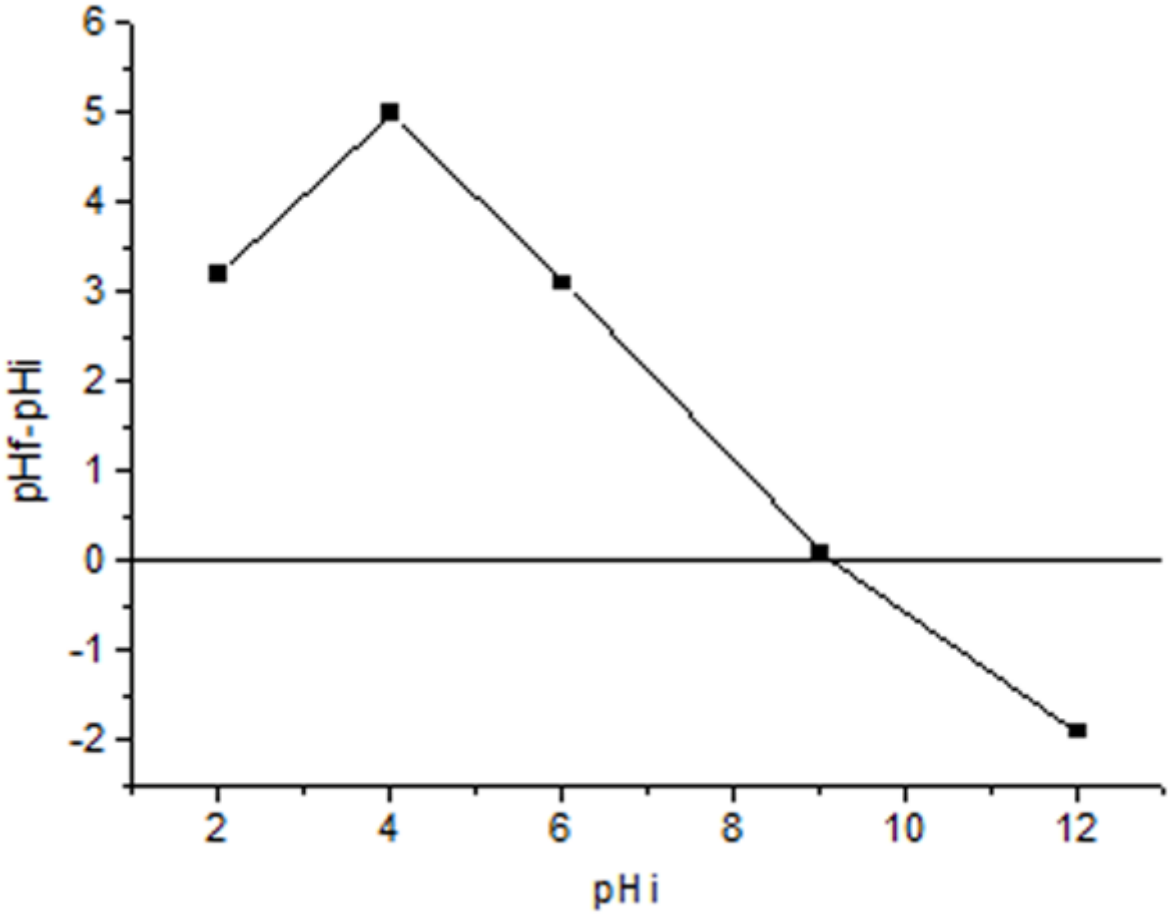

Figure 5

The pH_{PZC} of catalyst

Figure 6

Effect of pH value on the degradation of dye: $[Dye]_0$ = 100 mg/L, $[H_2O_2]_0$ = 27.6 mM, 0.01 g of catalyst and T = 20 °C

Figure 7

Effect of concentration of H_2O_2 on the oxidation of dye.[Dye]0 = 100 mg/L (100 ml), pH=3, 0.01 g of catalyst and T = 20 °C

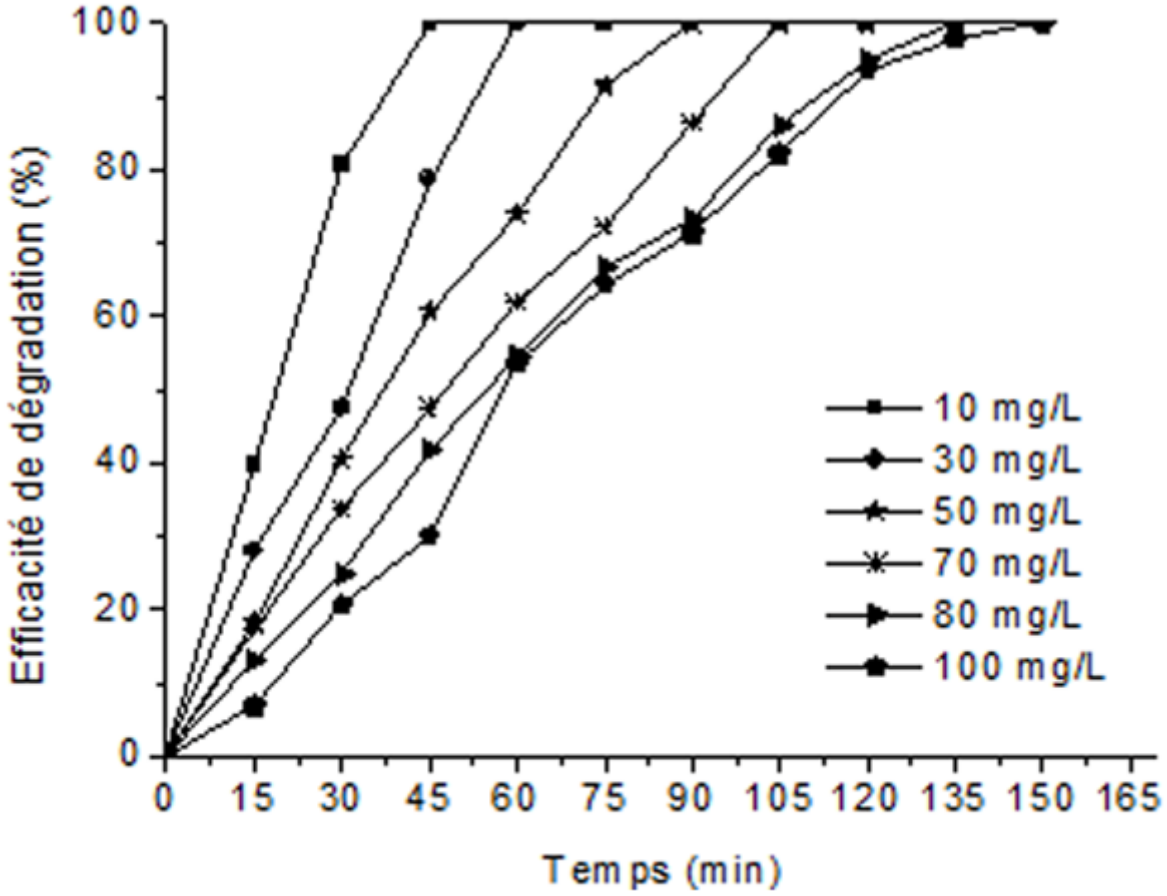

Figure 8

Effect of dye concentration. $[Dye]_0$ = 100 mg/L (100 ml), pH = 3, 0.01 g of catalyst and T = 20 °C

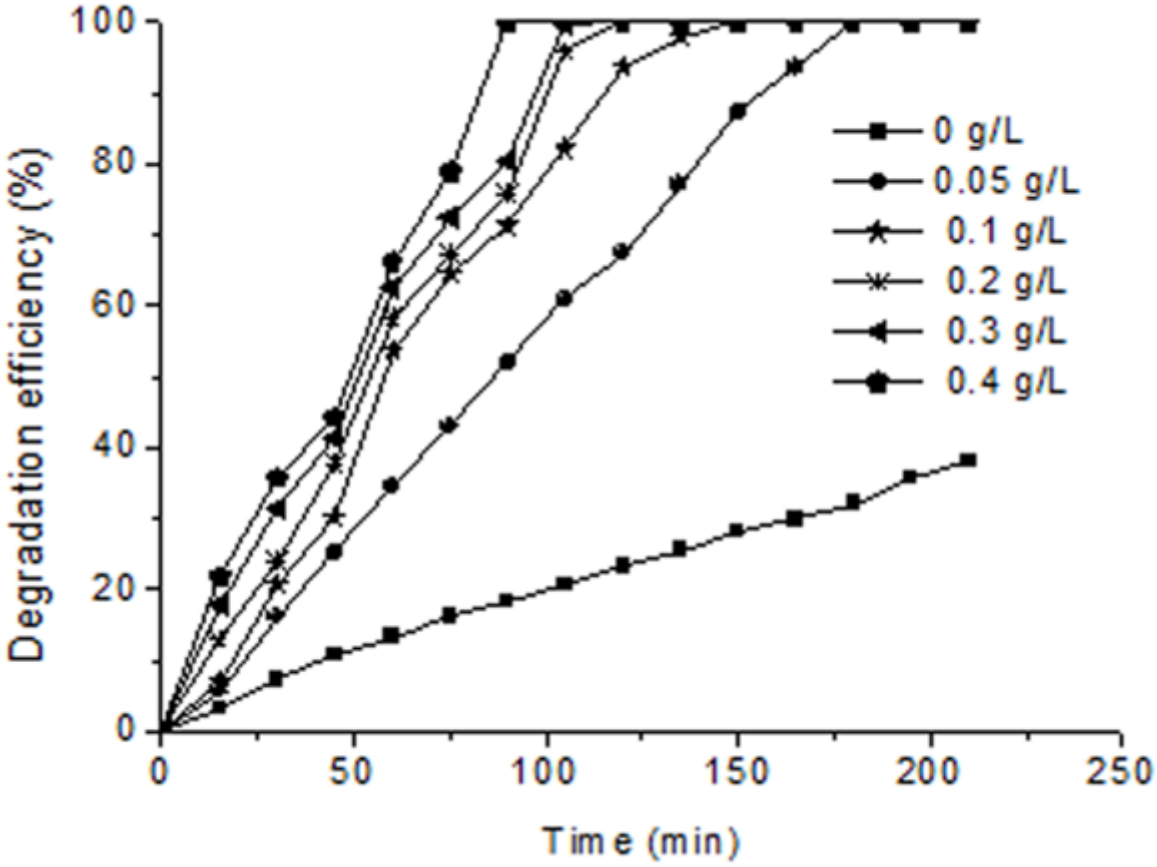

Figure 9

Effec%Mt of the catalyst dose. 100 ml of dye (100 mg/L), $[H_2O_2]_0$ = 27.6 mM, pH = 3 and T = 20 °C

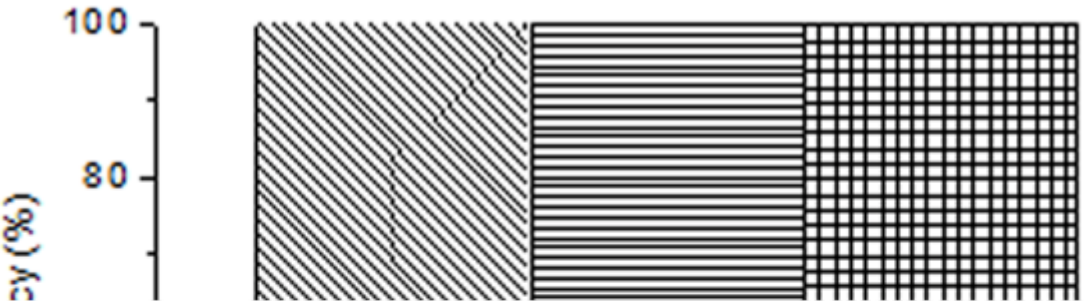

Figure 10

Reusability test of catalyst (Reaction conditions: 100 ml of dye (100 mg/L), $[H_2O_2]_0$ = 27.6 mM, pH = 3, T = 20 °C, in 240 min)

Figure 11

Temperature effect (Reaction conditions: 100 ml of dye (100 mg/L), $[H_2O_2]_0$ = 27.6 mM, pH = 3, 0.01 g of catalyst and T varies from 20 °C to 40 °C

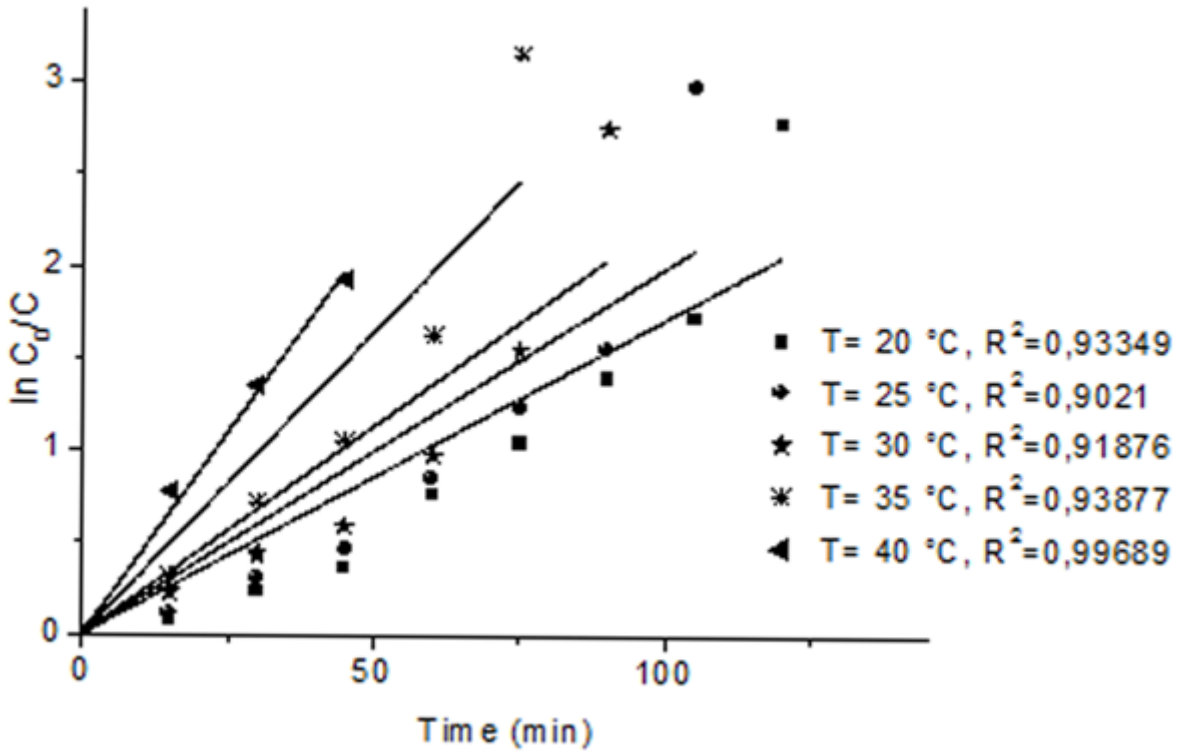

Figure 12

ln (C_0/C) versus time (t). (Reaction conditions: 100 ml of dye (100 mg/L), $[H_2O_2]_0$ = 27.6 mM, pH = 3, 0.01 g of catalyst

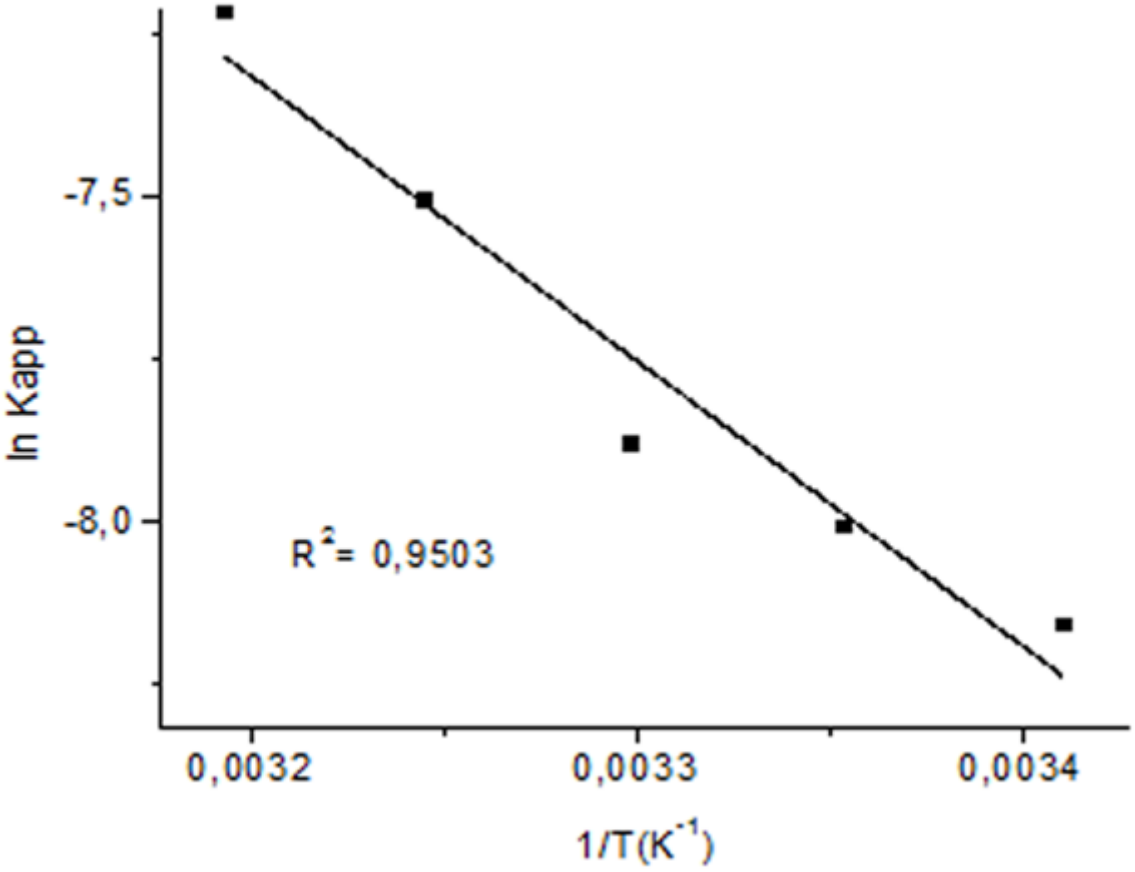

Figure 13

Validation of Arrhenius' law for the elimination of quinoline yellow by hydrogen peroxide in the presence of Cu/Fe

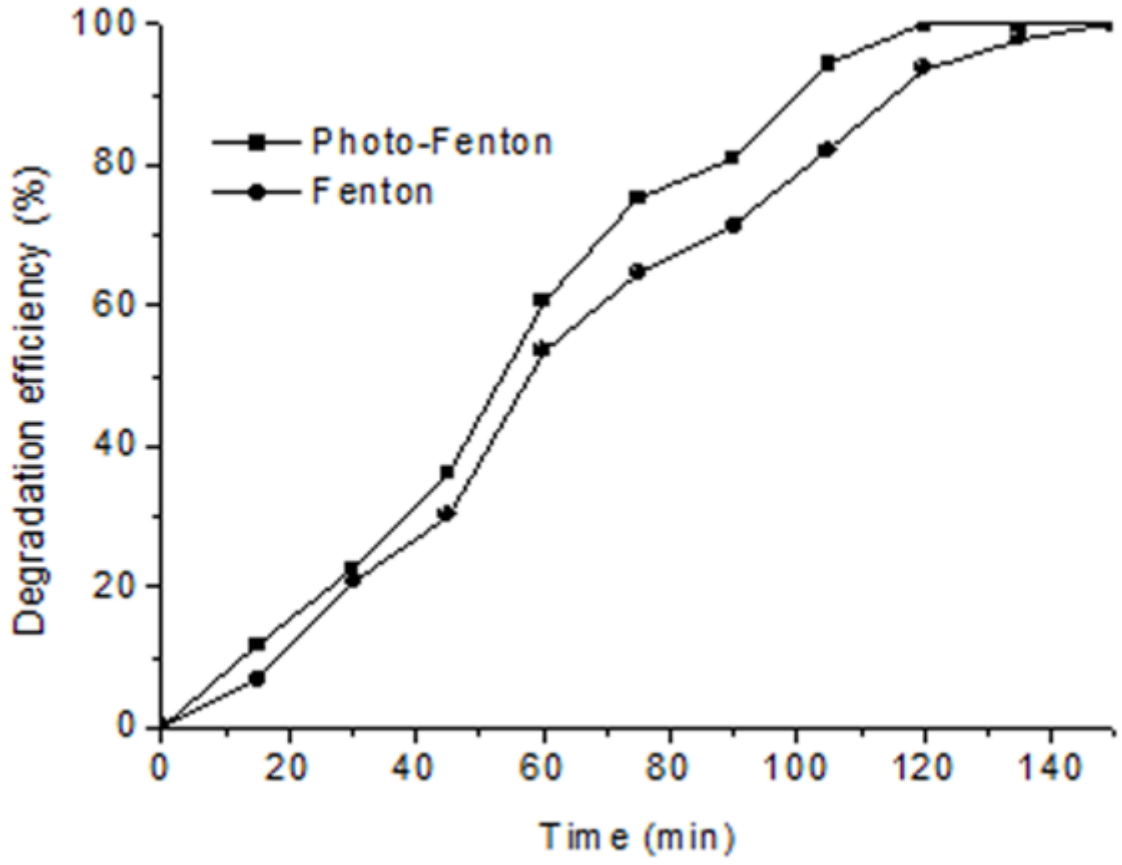

Figure 14

Comparative study of the degradation of the dye by Fenton and photo-Fenton systems under optimal conditions: $[Dye]_0$ = 100 mg/L (100ml), $[H_2O_2]_0$ = 27,6 mM, 0.01 g of catalyst and T = 20 °C

Supplementary Files

This is a list of supplementary files associated with this preprint. Click to download.

- GraphicalAbstract.png